A MARINE DEEP SEISMIC SOUNDING SURVEY OVER WINONA BASIN

by

ALLAN JAMES THORLEIFSON

B.A.Sc., University of British Columbia, 1976

A THESIS SUBMITTED IN PARTIAL FULFILLMENT OF

THE REQUIREMENTS FOR THE DEGREE OF

MASTER OF APPLIED SCIENCE

in

THE FACULTY OF GRADUATE STUDIES

(Department of Geophysics and Astronomy)

We accept this thesis as conforming

to the required standard

THE UNIVERSITY OF BRITISH COLUMBIA

July, 1978

In presenting this thesis in partial fulfilment of the requirements for an advanced degree at the University of British Columbia, I agree that the Library shall make it freely available for reference and study. I further agree that permission for extensive copying of this thesis for scholarly purposes may be granted by the Head of my Department or by his representatives. It is understood that copying or publication of this thesis for financial gain shall not be allowed without my written permission.

Department of Geophysics and Astronomy

The University of British Columbia
2075 Wesbrook Place
Vancouver, Canada
V6T 1W5

Date July 27, 1978

ABSTRACT

During the summer of 1975 a deep seismic sounding survey was carried out over Winona Basin, a deep water sedimentary basin located off the northern end of Vancouver Island. Three reversed refraction profiles were shot, one parallel and two perpendicular to the axis of the basin, with penetration from the ocean bottom to the upper mantle. Several sub-critical reflection profiles were also shot in an attempt to delineate the sedimentary structure of the basin.

The two sub-critical reflection profiles shot over the central part of the basin were analyzed using the T^2-X^2 method. The data sets gave layer velocities and thicknesses for 2 km of sediments for one of the profiles and .6 km for the other although petroleum industry data indicate that neither profile penetrated to the volcanic basement. The remaining reflection profiles were shot on the sides of the basin. On the western flank of Paul Revere Ridge, approximately 1 km of sediments with velocity in the range 2.5 to 3.5 km/s overlies volcanic basement. Over the continental slope on the east the seismic energy is strongly scattered below an upper 0.7 km of sediments.

Refraction profile 75-1,1R, along the axis of the basin, was analyzed in a previous study using synthetic seismograms. However, the severe lateral inhomogeneities across the basin necessitated the use of ray tracing for the cross basin refraction profiles, 75-2,2R and 75-3,3R. The final models are non-unique but they satisfy the seismic data very well and

are consistent with profile 75-1,1R, gravity data and current views on plate tectonics. They show deep crustal layers dipping from both sides of the basin towards the center.

Evidence for subduction as well as lateral motion between the Explorer and American plates has led to the conclusion that oblique subduction is occurring at Winona Basin.

TABLE OF CONTENTS

LIST OF TABLES

LIST OF FIGURES

ACKNOWLEDGEMENTS

For his encouragement and open helpfulness throughout all phases of this project I would like to thank my supervisor Dr. R.M. Clowes. I would also like to thank my fellow graduate students Henry Cheung, Andy Jurkevics and Barry Narod for their stimulating discussions and helpful suggestions. Special thanks also go to Ken Whittall for his enthusiastic work with the ray tracing program. Chevron Standard Ltd. provided the opportunity to examine their reflection record sections in Winona Basin.

I would also like to express my appreciation to the officers and crew of the C.F.A.V. ENDEAVOUR and C.F.A.V. LAYMORE as well as the explosives experts from the Fleet Diving Unit, Pacific Maritime Command, Esquimalt, B.C. for their assistance during the cruise.

Funding for this project was provided through a research contract and research agreements with the Geological Survey of Canada, Department of Energy, Mines and Resources and through operating grant A7707 of the National Research Council of Canada. Additional funds were supplied by Mobil Oil Canada Ltd., Shell Canada Resources Ltd. and Chevron Standard Ltd.

1. INTRODUCTION

The western Canadian continental margin is tectonically a very complex area. A series of active sea-floor spreading ridges connected by transform faults separates the oceanic crust into the Pacific plate to the west and the much smaller Explorer and Juan de Fuca plates to the east; east of the latter plates is the large North American plate, the western part of which has continental crust (see Fig. 1.1). The Explorer and Juan de Fuca plates are remnants of the once larger Farallon plate, and are now separated into two sub-plates by the Nootka Fracture Zone (Riddihough and Hyndman, 1976; Hyndman, personal communication, 1977). North of the Dellwood Knolls, lateral motion occurs between the Pacific and North American plates along the Queen Charlotte transform fault zone; south of the Dellwood Knolls, convergence of the North American plate with the Explorer and Juan de Fuca plates results in compression of the oceanic crust and subduction of the oceanic plate beneath the continental plate (Riddihough and Hyndman, 1976). The point along the continental margin which separates the transform fault motion from the convergent motion is known as the triple junction between the three plates. The change in position of this triple junction over the past several million years is believed to be at least partially responsible for many of the prominent features of the region, including Winona Basin, the area of interest for this deep seismic sounding survey.

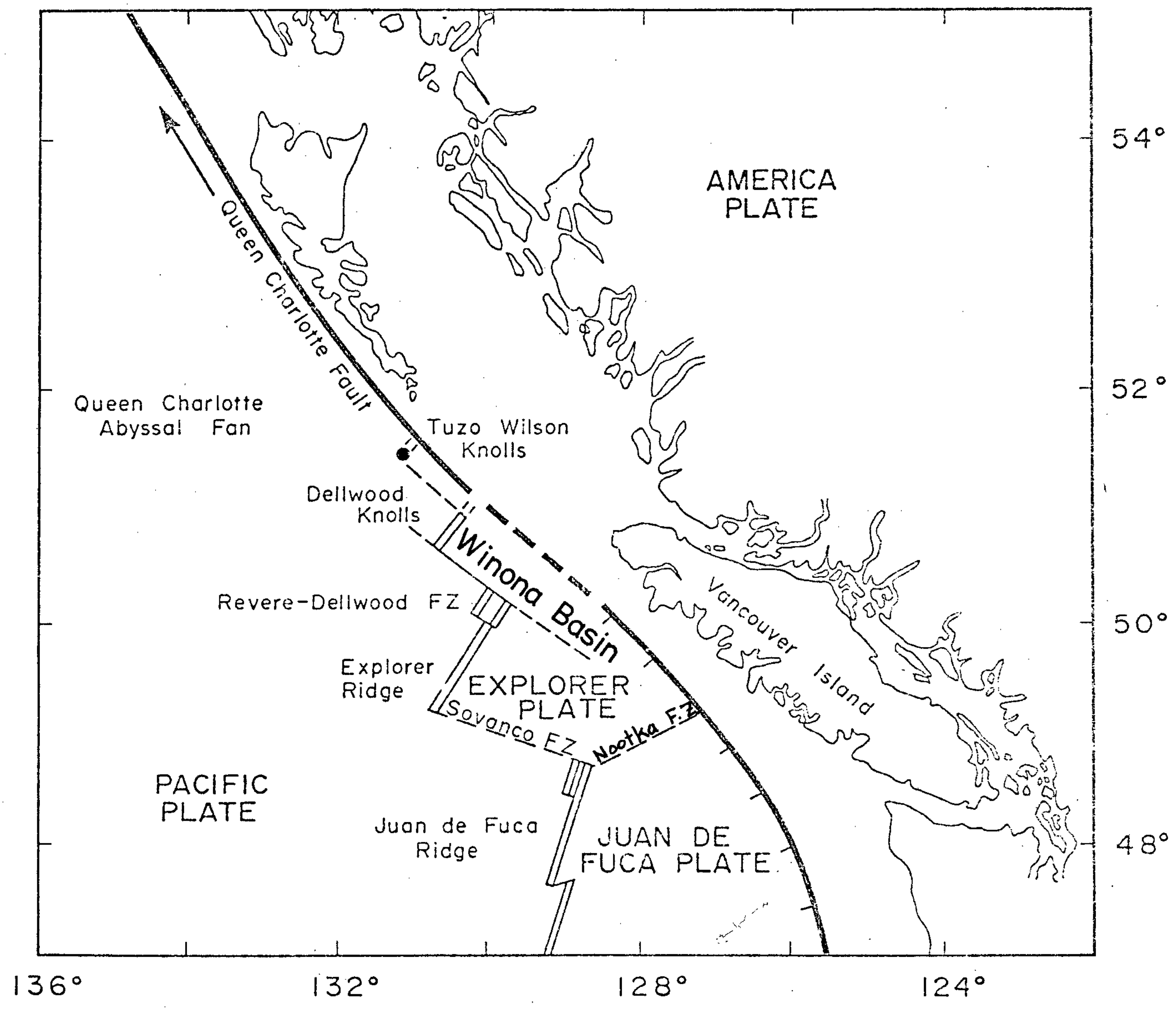

Fig. 1.1 Location of Winona Basin with respect to the general tectonic features off Canada's west coast.

1.1 STRUCTURE AND TECTONICS OF WINONA BASIN

Winona Basin is a deep water sedimentary basin located at the foot of the continental slope off the northern tip of Vancouver Island (see Figs. 1.1 & 1.2). It is bounded by Paul Revere Ridge to the southwest, the Brooks Fracture Zone (adjacent to Brooks Peninsula) to the southeast and the Dellwood Knolls to the northwest. The basin itself, which is generally believed to be of Pliocene-Pleistocene age, is divided into two smaller basins by Winona Ridge, which runs obliquely down the length of the basin.

A -160 mgal free air gravity anomaly located over the eastern portion of the basin has been interpreted by Couch (1969) as being due to 4 to 6 km of sediments. Petroleum industry seismic reflection data (Chevron Standard Ltd., Calgary, unpublished data) indicate up to 4 km of sediments. The basin does not show the typical linear magnetic anomaly patterns associated with sea floor crust which has been formed at a spreading center, but Riddihough (personal communication, 1978) has suggested that the overlying sediments could obliterate such a pattern.

Winona Basin is located near the junction of the Pacific, American, and Explorer plates and the main features of the basin have almost certainly been controlled by the complex interaction of spreading ridge readjustment and subduction at the continental margin. In a study of the magnetic anomaly patterns of the area, Riddihough (1977) has shown that readjustment of spreading rates and directions over the past

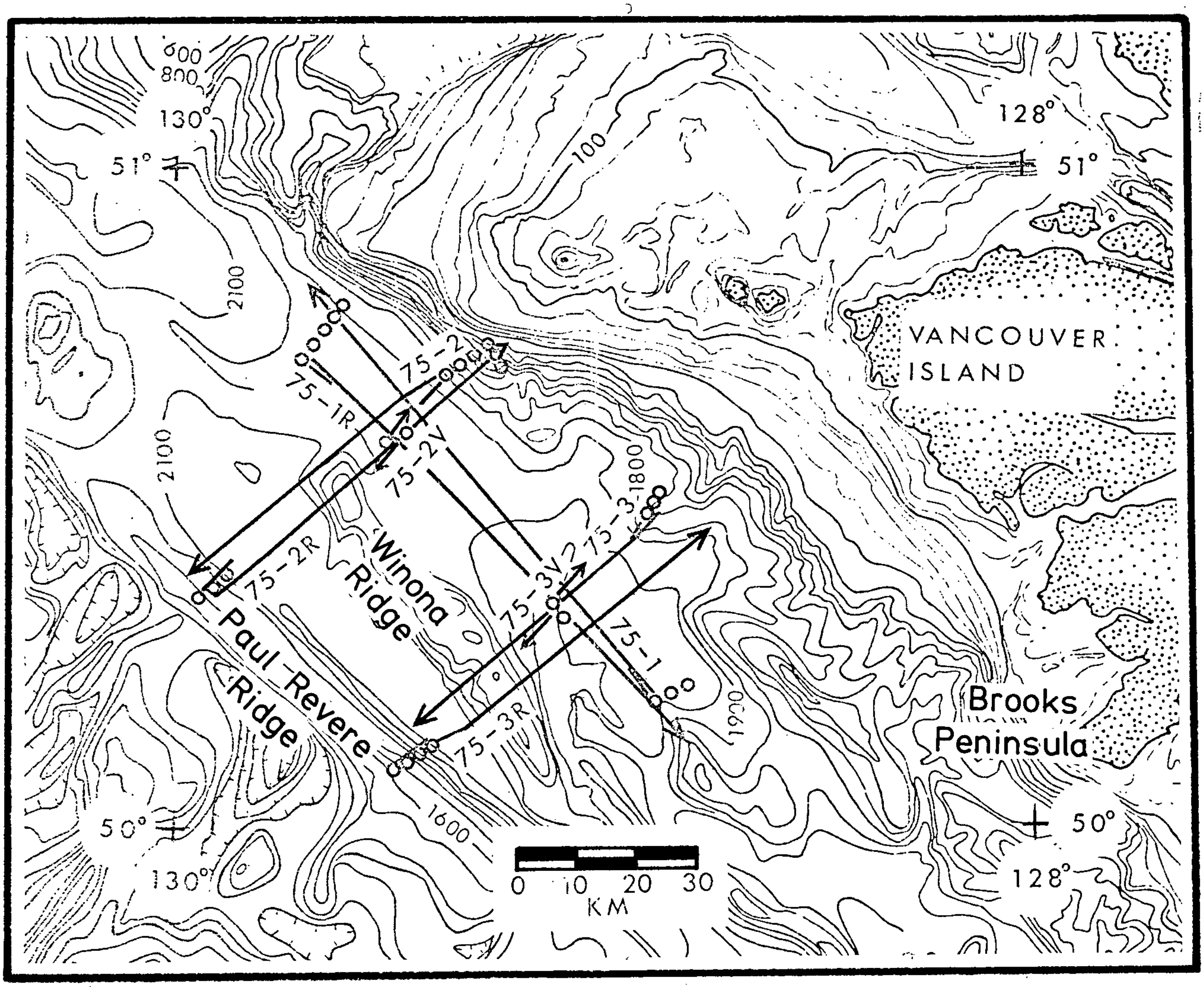

Fig. 1.2 Location of 1975 marine deep seismic sounding profiles in Winona Basin. Open circles show the drift track of the receiving ship during the profile runs. Profiles 75-2, 75-2R, 75-2V, 75-3, 75-3R and 75-3V are the subject of this study. Bathymetric contours are in meters. (from Tiffin and Seemann, 1975)

10 million years has resulted in a complicated motion of the triple junction near the area of Brooks Peninsula. This has also been suggested by Murray and Tiffin (1974) based on evidence of subduction to the southeast of the Brooks Fracture Zone and strike-slip motion to the northwest. If the triple junction is now located at the Dellwood Knolls, it must have migrated northward over the past few m.y. resulting in the formation of Winona Basin. It was suggested by Hyndman and Riddihough (personal communication, 1978) that the triple junction may have migrated along Winona Ridge, which lines up well with the Queen Charlotte Fault, rather than following the indentation in the coast off northern Vancouver Island. This would imply that the eastern portion of the basin was at least temporarily stuck to the continental plate resulting in the east side of the basin being considerably older than the west. However Davis (personal communication, 1978) has shown, on the basis of heat flow measurements, that both sides of the basin are not likely more than 6 m.y. old.

Another possibility is that Winona Ridge, from which consolidated sediments have been dredged (Chase, personal communication, 1978), was formed by slow convergence of the oceanic and continental plates. The newly formed oceanic crust, being thin and still relatively warm, may have been more susceptible to deformation and compression than to subduction. Since there very likely is subduction to the southeast of the basin and definitely strike-slip motion to the northwest (Tiffin et al, 1972; Chase et al, 1975; Riddihough and Hyndman, 1976), the northwestern edge of the subducting plate must be either beneath, or just southeast of the basin. Riddihough (1977) shows it as being just southeast of the basin. Continuous seismic profiles (C.S.P.'s) show the volcanic basement dipping beneath Winona Basin from Paul Revere Ridge (see Figs. 1.3 & 1.4), but it is not clear if this is actually a subducting plate or just the result of deformation and uplift along Paul Revere Ridge.

1.2 PROJECT DESCRIPTION

In order to gain a further understanding of the significance of Winona Basin, a seismic survey was carried out during the summer of 1975. The objective of the study was to provide detailed velocity and structural information for the crust and upper mantle in the area. Three reversed profiles were run; one along the center of the eastern portion of the basin and two across the basin (see Fig. 1.2). To gain further information about the sediments, short near vertical incidence profiles were run at the intersections of the cross profiles with the long profile. The marine seismic system (Clowes, 1977) records near vertical incidence to wide-angle reflected and refracted waves with penetration from the ocean bottom to the upper mantle.

The first 16 shots of each profile were set at shallow depths (7 m) in hopes that the gas bubble would blow out at the surface, minimizing the bubble pulse problem. The shooting ship then returned to its starting point and proceeded to shoot the entire profile with the shots at the

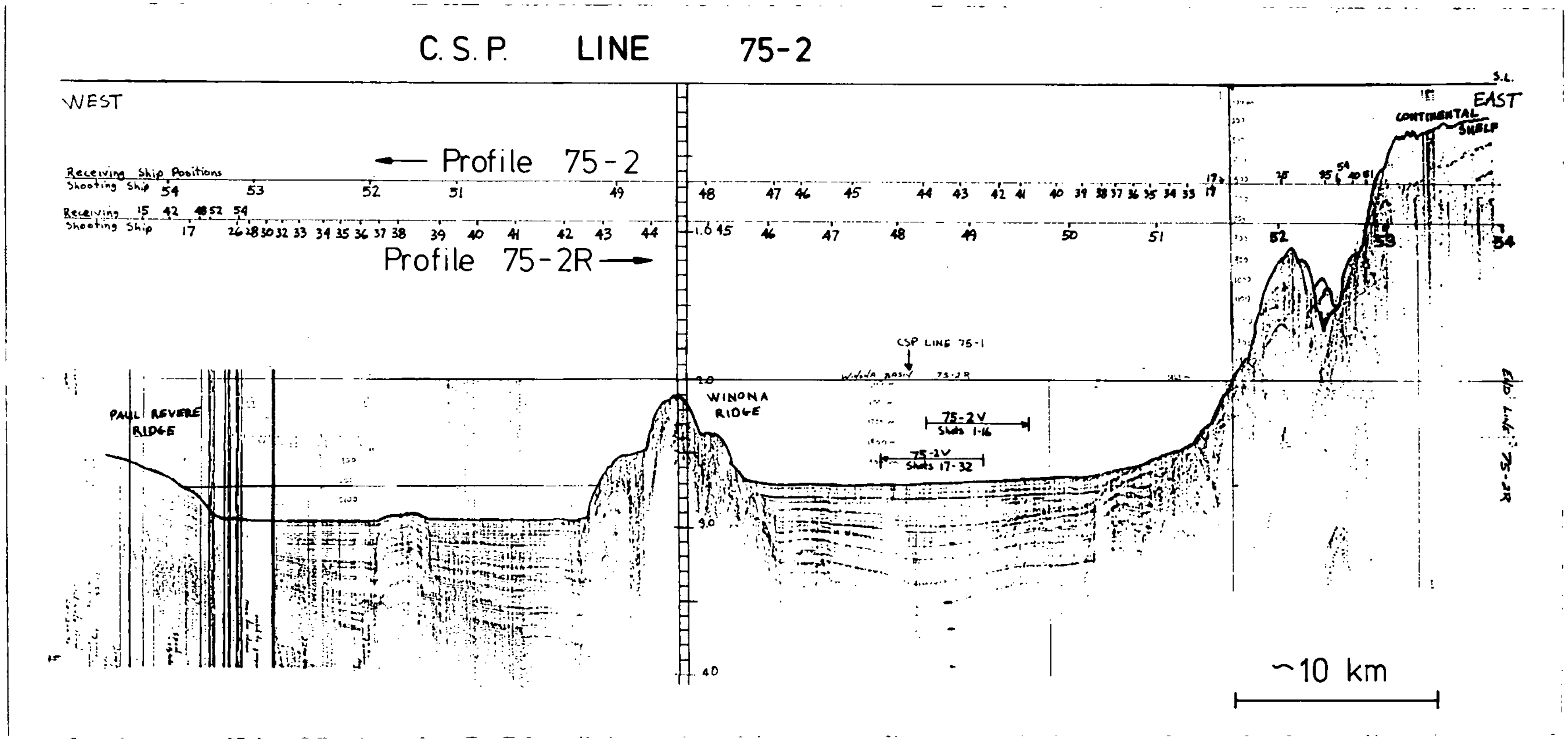

Fig. 1.3 Continuous seismic profile line 75-2, parallel to refraction line 75-2R. Superimposed above the section are profile lines showing approximate shot locations (numbers below the lines) and receiving ship locations for these shots (numbers above the lines).

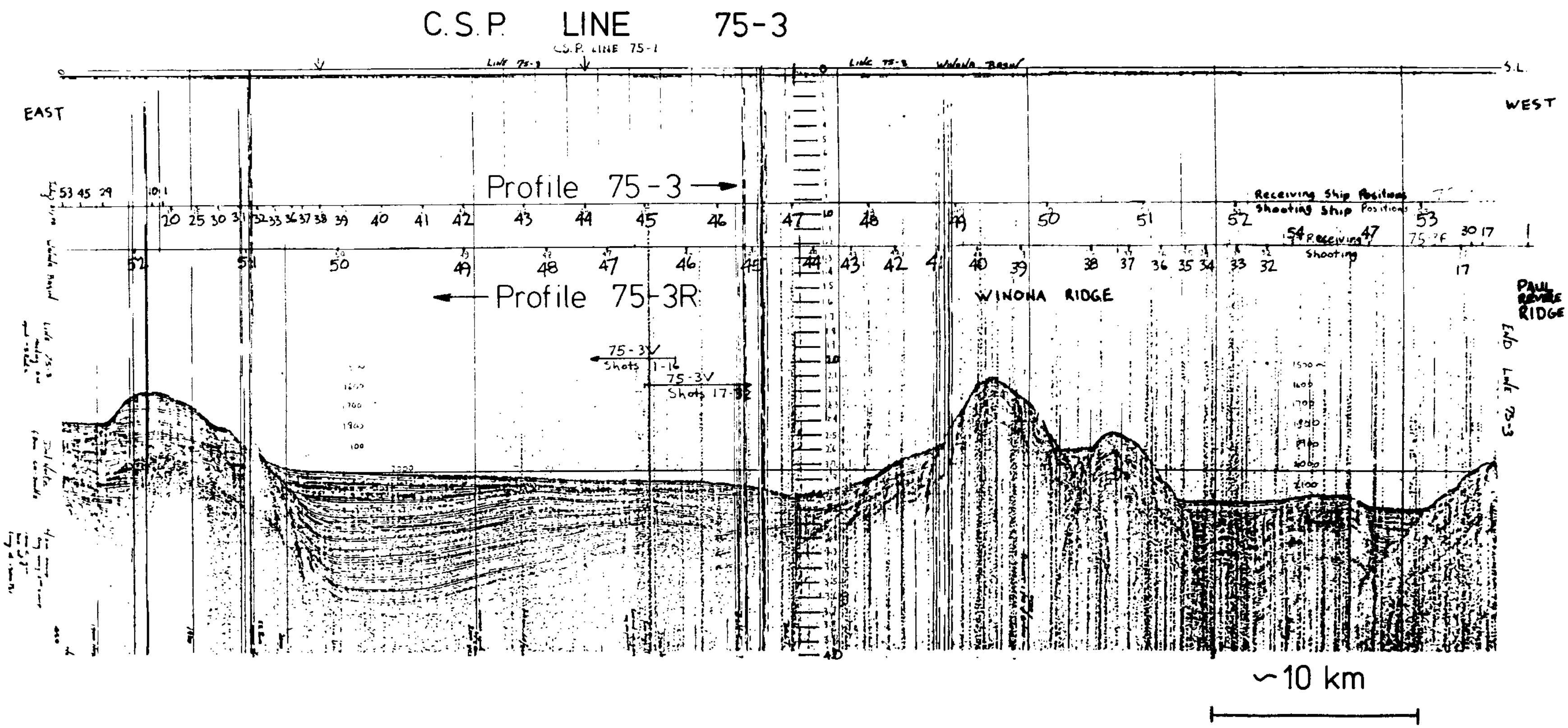

Fig. 1.4 Continuous seismic profile line 75-3, parallel to refraction line 75-3. For description of profile lines see Fig. 1.3.

optimum depths for maximum penetration of seismic energy, these depths depending on the charge size (Shor, 1963).

Profiles 75-1 and 75-1R were analyzed by Lynch (1977) while this thesis presents an analysis of profiles 75-2, 75-2R, 75-3, 75-3R, 75-2V and 75-3V. Since the results of Lynch's work are an integral part of this study, many references will be made to his thesis.

2. DATA ACQUISITION AND PRELIMINARY ANALYSIS

2.1 DATA ACQUISITION

A detailed description of the marine deep seismic sounding system is given by Clowes (1977). It is similar in principle to the two-ship refraction technique described by Shor (1963), in which one ship, the recording ship, drifts freely at one end of the line while the second ship proceeds along a predetermined course releasing explosive charges. For our survey, ship positions were determined by LORAN A.

On the receiving ship, the seismic signals were detected by six hydrophones suspended to a depth of 45 m from a 610 m cable. The signals were pre-amplified at the hydrophone, filtered from 0.8 to 100 Hz and then amplified by individual amplifiers manually set for each shot. The six analog signals plus WWVB time code were digitized at 312.5 Hz and written onto magnetic tape using an I.B.M. compatible, 14 bit, multi-channel data acquisition system (see Clowes, 1977). Five data channels plus the WWVB time code were monitored on a 6-channel chart recorder for quality control.

On the shooting ship, the direct water wave (D.W.W.) was detected by both a hydrophone trailed directly behind the ship and a geophone located on deck. These two signals plus the WWVB time code were recorded on a 4-channel FM tape transport while the hydrophone and WWVB signals were recorded directly onto a 2-channel high speed Brush chart recorder. For the profiles being analyzed in this thesis, the charges ranged in size from 2.3 kg to 96 kg of Geogel, a commercial explosive, and were suspended at optimum depths by large red balloons. The shot-to-ship distances were measured with a rangefinder focussed on the balloons.

2.2 PRELIMINARY ANALYSIS

1) Demultiplexing

Since the six seismic channels plus WWVB time code were recorded digitally in multiplexed form, the first data processing step was demultiplexing. The analog records, on which a marker channel identified the time interval for digitization, were used to edit out unnecessary data since several seconds were recorded both before and after the arrival of the shot energy. A computer program written by Lynch (1977) was used to perform the demultiplexing. The program checked the input tapes for missed data and tape errors and wrote the corrected, demultiplexed data onto new magnetic tapes. The six seismic channels plus WWVB time code for a single shot comprise one data file.

2) Shot Origin Times

The D.W.W. recorded at the shooting ship was used to determine the shot origin times. The arrival of the signal at the hydrophone could be timed to better than 5 ms from the 2-channel chart recordings. Since the charges were detonated at various depths and distances from the shooting ship, corrections were made for the travel time, generally of the order of 100 ms, from shot to ship. This introduced a further 15 to 20 ms error.

3) Shot-Receiver Distances

The shot to receiver distances were determined by measuring the D.W.W. travel time and assuming a constant water velocity of 1.49 km/s. To measure the arrival time of the D.W.W., the six seismic and WWVB time channels were plotted with a common time origin at a rate of .126 s/cm (.32 s/inch), each channel being normalized to a maximum amplitude of 1.9 cm (see Fig. 2.1). The error in measuring the D.W.W. arrival is 10 - 20 ms and combined with origin time errors this gives a total error in distance of the order of 50 - 80 m.

4) Topographic Correction

As can be seen from the C.S.P. records (Figs. 1.3 & 1.4), it was necessary to make corrections for topography. Since the eastern portion of the basin is at a uniform depth of approximately 2.0 km, all travel times were corrected to this depth. A velocity of 2.0 km/s was assumed for the immediate sub-bottom material, this being representative of shallow sediments. The effect of this correction is to replace all sub-bottom material above 2.0 km depth with 1.49 km/s material, and all water below 2.0 km with material of velocity 2.0 km/s. The correction is

$$\Delta T = H\left(\frac{1}{V_w} - \frac{1}{V_s}\right) / \cos\theta \qquad (2.1)$$

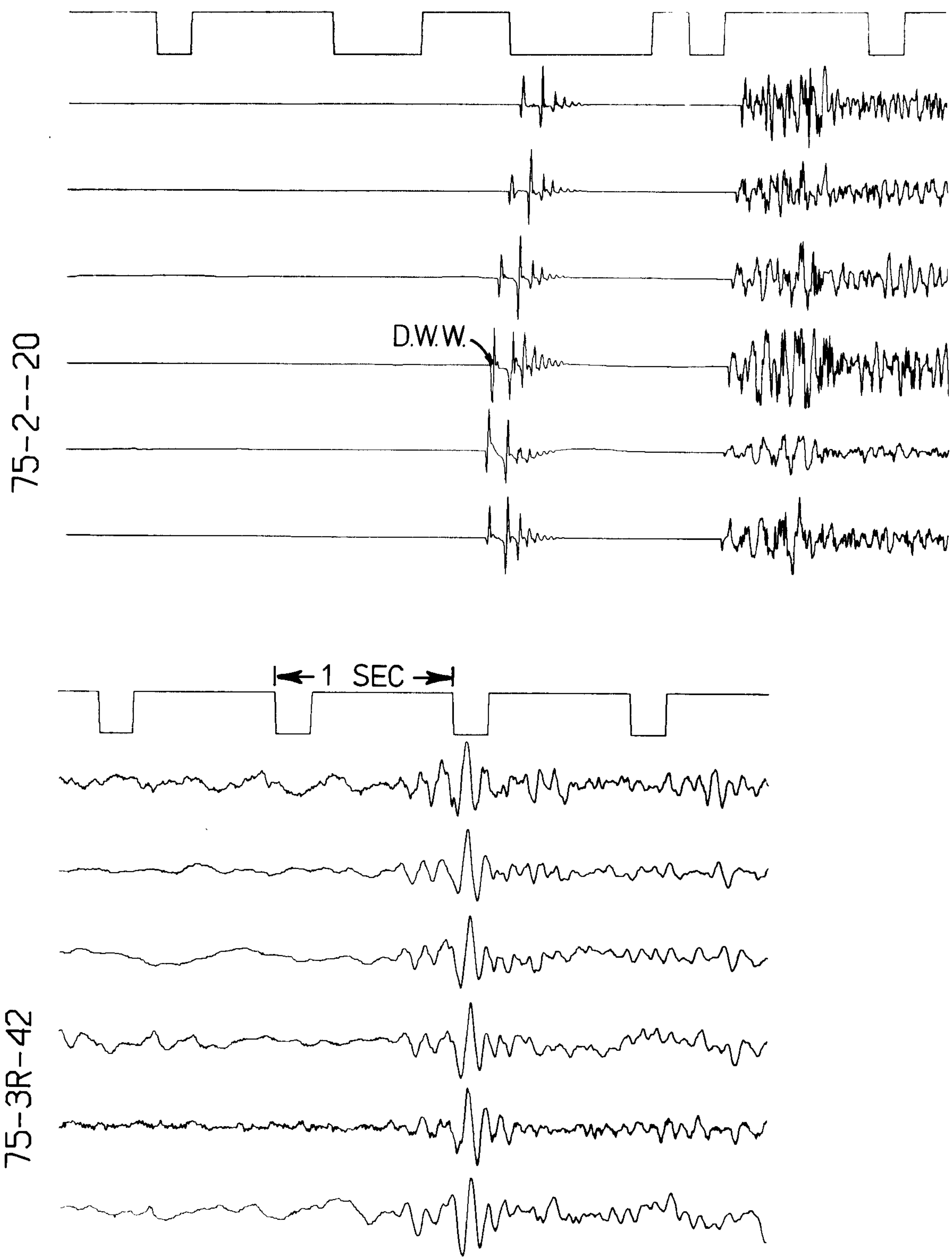

Fig. 2.1 Two seismograms typical of those used to time the direct water wave (D.W.W.) and the first refraction arrivals. The bubble pulse sequence is clearly visible following the D.W.W. arrival on the upper set of traces. The lower set of traces shows the arrival of refraction energy at a distance of 19 km.

where H is the height of the topography from 2.0 km depth, V_w is the water velocity, V_s the sub-bottom velocity and θ the angle of the ray from vertical. This correction, which is approximately 50 ms for 250 m of topography, was applied to both the shooting ship and the receiving ship water depths. Since the two sides of the basin are close to 2.0 km depth, the greatest effect of the topographic correction is over Paul Revere Ridge, Winona Ridge and the continental shelf and slope. The velocities beneath these areas are not well known so that the corrections could be in error. For example, if 1.0 km of continental slope material is corrected at 2.0 km/s the correction is 170 ms, while if it is corrected at 4.0 km/s the correction is 420 ms. This must be considered when analyzing such areas.

During the survey there was no depth recording equipment operating on either ship, although a request for working echo sounders had been made prior to the cruise. In order to obtain depth information, a chart produced by the Canadian Hydrographic Service was used. On this chart are plotted water depths along an extensive series of ship tracks. The major source of error in determining the depths below our ships from this chart is the uncertainty in ship position, which for LORAN A in the region of our survey is of the order of 1 km.

It was also possible to calculate the depths below the shooting ship by measuring the difference in travel time of the D.W.W. and the first water-bottom bounce. Consider the following diagram:

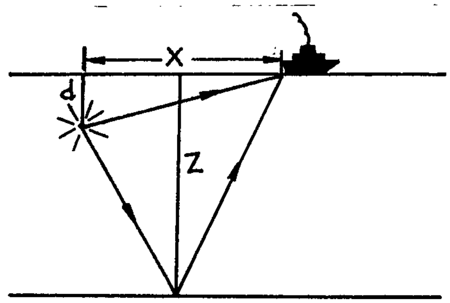

If T_1 is the arrival time of the D.W.W. and T_2 the arrival time of the water-bottom bounce then, assuming near-vertical incidence,

$$T_1 = \sqrt{X^2 + d^2}/V_w \qquad (2.2)$$

$$T_2 \cong \left(2\sqrt{\left(\tfrac{X}{2}\right)^2 + Z^2} - d\right)/V_w \qquad (2.3)$$

where X is the horizontal distance, d the shot depth, and Z the water depth. Let $\Delta T = T_2 - T_1$, then

$$Z = \sqrt{\left(V_w \Delta T + d + \sqrt{X^2 + d^2}\right)^2 - X^2}/2 \qquad (2.4)$$

The uncertainty involved should be no more than 30 m over a depth of 2000 m. The results obtained using this method agree very well with those taken from the bathymetric chart so it was assumed that the receiving ship depths taken from the chart were reasonable as well.

5) Record Sections

In order to present the data in the best possible way for interpretation, a record section was produced for each profile. The program used to compile the record sections makes corrections for amplifier gain, charge size, spherical spreading, and hydrophone sensitivities (see Lynch, 1977). The correction for charge size is $W^{-1/3}$ for a weight of W pounds (O'Brien, 1960; Muller et al, 1962) and the correction for spherical spreading is X^2 for head wave amplitudes at large distances (Cerveny and Ravindra, 1971) and X for reflection amplitudes. Such amplitude scaling with distance gives a record section with amplitudes normalized such that arrivals at all distances can be seen clearly. The program also contains a zero phase, four pole Butterworth filter (Kanasewich, 1976) which was used primarily to reduce high frequency noise.

3. SUB-CRITICAL REFLECTION DATA

3.1 METHODS OF ANALYSIS

All reflection profiles were interpreted by first "picking" the arrival times vs. distance for all reflecting horizons which could be identified. However, differences in individual profiles made it necessary to use two methods of analysis. Profiles 75-2V and 75-3V were shot as split-dip profiles (Telford et al, 1976) and it is obvious from the C.S.P. records that there is very little dip in the layering. Profiles 75-2, 75-2R, 75-3 and 75-3R on the other hand, are not split-dip profiles and it is obvious from the C.S.P. records that there is significant dip in the horizons over which they were shot. For these reasons, profiles 75-2V and 75-3V were analyzed using the standard T^2-X^2 method for flat layers and the other profiles were analyzed using the equation for dipping layers.

1) T^2-X^2 Method

For plane, horizontal reflecting horizons in a multilayered medium, the approximate relationship between travel time T and distance X is

$$T^2 = \frac{X^2}{\bar{V}^2} - T_o^2 \tag{3.1}$$

where $\bar{V}$ is the average rms velocity down to a horizon and T_o the 2-way vertical incidence travel time. The right-hand side of equation 3.1 consists of the first two terms of a Taylor series expansion for $T^2(X)$ about the point $X=0$. A plot of T^2 vs X^2 will yield a slope of $1/\bar{V}^2$ and an intercept of T_0^2.

For the case of several layers, Dix (1955) gives the interval velocity V_K as

$$V_K = \sqrt{\frac{\bar{V}_K^2 T_K - \bar{V}_{K-1}^2 T_{K-1}}{T_K - T_{K-1}}} \tag{3.2}$$

where $\bar{V}_K$ and T_K are the average rms velocity and 2-way vertical incidence travel time to the bottom of the k^{th} layer. The thickness of the k^{th} layer is then given by

$$h_K = V_K \left(\frac{T_K - T_{K-1}}{2}\right) \tag{3.3}$$

2) Dipping Layer Approach

The relationship between travel time and distance for a dipping plane horizon is, (from Telford et al, 1976)

$$T^2 = T_0^2 \left\{ 1 + \frac{(X^2 + 4hX\sin\theta)}{4h^2} \right\} \tag{3.4}$$

where θ is the angle of dip, and h is the thickness normal to the bed at the origin.

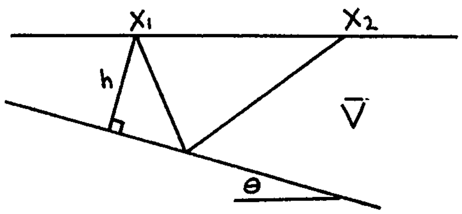

Consider 2 points, T_1 and T_2 with corresponding X_1 and X_2, from a travel time curve. For convenience choose $X_1=0$, in which case $T_1=T_0=2h/\bar{V}$, the travel time intercept. Therefore,

$$T_1^2 = T_0^2 \tag{3.5}$$

$$\begin{aligned} T_2^2 &= T_0^2\left\{1 + \frac{(X_2^2 + 4hX_2\sin\theta)}{4h^2}\right\} \\ &= T_0^2 + \frac{X_2^2}{\bar{V}^2} + \frac{2T_0X_2\sin\theta}{\bar{V}} \end{aligned} \tag{3.6}$$

Let $\Delta T^2 = T_2^2 - T_1^2$, then

$$\bar{V}^2 - \frac{(2T_0X_2\sin\theta)}{\Delta T^2}\bar{V} - \frac{X_2^2}{\Delta T^2} = 0 \tag{3.7}$$

In this equation there are two unknowns, $\bar{V}$ and θ. In order to find $\bar{V}$, θ must be known. Fortunately we can estimate θ from the C.S.P. records, although only the first sub-bottom layer can be analyzed with any degree of accuracy.

Again, the Dix formula can be used to find the interval velocity, which in turn can be used to find the layer thickness.

3.2 BUBBLE PULSE DECONVOLUTION

In marine seismic operations, the source signature produced by the explosive energy source is a series of impulses caused by the repeated cycle of gas bubble expansion and contraction (see Kramer et al, 1968). For sub-critical reflection data this wavelet can seriously complicate the profile interpretation.

An attempt was made to reduce the bubble pulse problem by deconvolution filtering. Two methods were tried, both requiring a detailed knowledge of the source signature. The first method was divisional deconvolution using the water-level parameter (Clayton, 1975). The second method was a technique devised by Wood et al (1978), which consists essentially of cross-correlating the trace with the source signature. The trace should then contain the autocorrelated source signature which can be processed into a desired shape by an optimum lag Wiener inverse filter. The advantage of this procedure is that the autocorrelation function has a zero phase spectrum, while the original bubble pulse signature is mixed delay, which causes problems when using the conventional Wiener spiking filter method.

When applied to the data, both filters produced no noticeable improvement. This is most likely because no true source signatures were available. Instead, what was used was the arrival at the receiving ship of the D.W.W. which is complicated by the ghost arrival from the water surface.

A deconvolution method which does not depend on source signatures would probably give better results. Such a method is Minimum Entropy Deconvolution (Wiggins, 1977) which is based on searching each trace for sequences which have identical moveout. This method was not attempted here because of time limitations and also because for most arrivals the bubble oscillations did not present a severe problem. For later arrivals it is unlikely that deconvolution would significantly improve matters, because of the lower signal to noise ratios encountered. The main advantage would be the enhancement of primary arrivals within 500 ms of the water bottom arrival.

3.3 ANALYSIS OF RESULTS

1) Profiles 75-2V and 75-3V

Profiles 75-2V and 75-3V were both shot as split-dip profiles. The receiving ship drifted freely while the shooting ship released explosives, first in one direction from the receiving ship, and then in the opposite direction. All shots were detonated at 7 m depth.

The record section for the eastern half of 75-2V is shown in Fig. 3.1, with all traces filtered from 5 to 30 Hz. The record section for the western half is virtually identical to that for the eastern half, indicating little or no dip in the reflecting surfaces. This agrees with the C.S.P. record (Fig. 1.3) which shows relatively flat lying sediments in this area of the basin. The first strong arrival of energy is the water bottom bounce from the initial explosive impulse. The next strong arrival corresponds to the bottom bounce from the first oscillation of the gas bubble created by the underwater explosion. The bottom bounce arrivals from the second and third bubble oscillations are also present, but at reduced amplitudes. The long bubble train greatly complicates the record, but because the bubble pulses have an identical

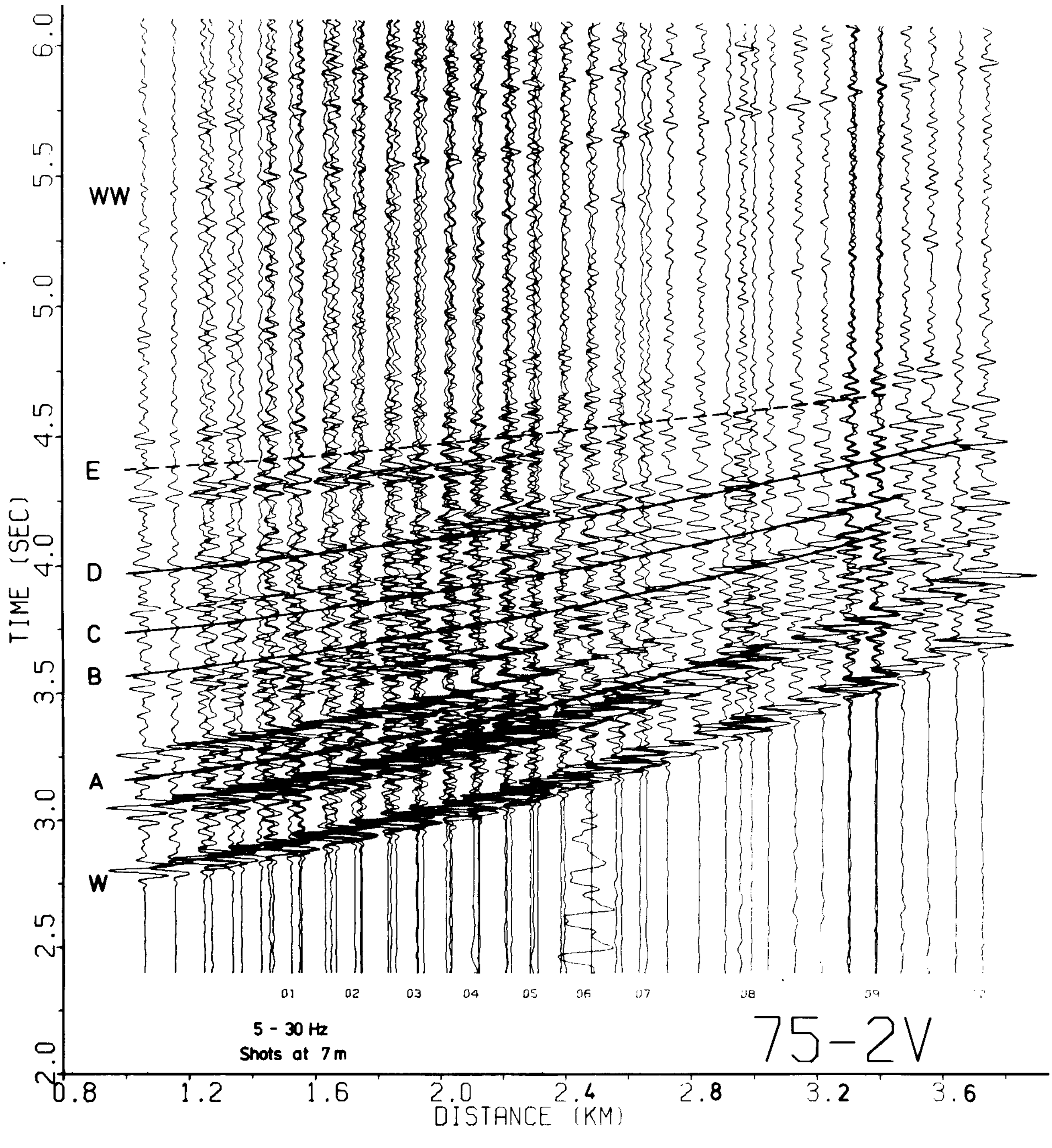

Fig. 3.1 Record section for reflection profile 75-2V. All traces have been filtered from 5 to 30 hz. The water bottom reflection is marked W and is followed 250 ms later by the water bottom reflection of the first bubble pulse. A, B, C, and D are clear primary reflections while E is less certain. WW is the first order multiple of W.

moveout to the initial impulse for a given reflector, it is possible to identify arrivals from deeper horizons by their different moveouts. Furthermore, since the time interval

Table I Reflection interpretation results for profiles 75-2V and 75-3V.

Profile	Layer	Velocity (km/s)	Thickness (km)	Depth (km)
75-2V	W	1.49	2.00	2.00
	A	1.62	.33	2.33
	B	1.83	.39	2.72
	C	2.04	.18	2.90
	D	2.49	.30	3.20
	E	3.63	.77	3.97
75-3V	W	1.49	2.05	2.05
	A	1.67	.40	2.45
	B	2.03	.20	2.65

between each successive bubble pulse decreases along the bubble train, it is nearly always possible to determine the position of an arrival along the train by measuring the time interval to the nearest arrival with identical moveout. By identifying all prominent arrivals in this manner it was possible to distinguish clearly the four sub-bottom reflectors A, B, C and D shown in Fig. 3.1. A fifth set of arrivals, labeled E, shows a distinctly different moveout than D but is partially obscured by both noise and bubble oscillations from earlier arrivals. However, the first bubble pulse of E, 250 ms after the event marked, can be correlated across most of the section and gives credence to the existence of this reflector. The T^2-X^2 results for these five layers are given in Table I. Beyond E there appear to be additional sets of coherent arrivals; however the calculated interval velocities for these are much too low, indicating that they are most likely reverberations from earlier arrivals. But at a time of 5.25 s, there is an event with small moveout, not clear enough for analysis, which suggests at least one deeper reflector. At approximately 5.4 s the first set of water bottom multiples is clearly visible; it obscures any possible deep crustal reflections.

The record section for the western half of profile 75-3V is shown in Fig. 3.2. Only two sets of primary arrivals, A and B, are identified, with virtually no coherent energy after 3.5 s. This is consistent with the C.S.P. record (Fig. 1.4) and petroleum industry reflection data which show deformed sediments with no continuous layering below about 3.5 s. There is some possibility of a primary arrival between W and A, but it is so badly obscured by bubble oscillations that it cannot be positively identified. The record section for the eastern half of 75-3V is similar to that of the western half except the arrivals are even more obscured by bubble oscillations. Since the C.S.P. record shows very little dip in the layering, only the record section for the western half of the profile was used in the analysis. The results are summarized in Table I.

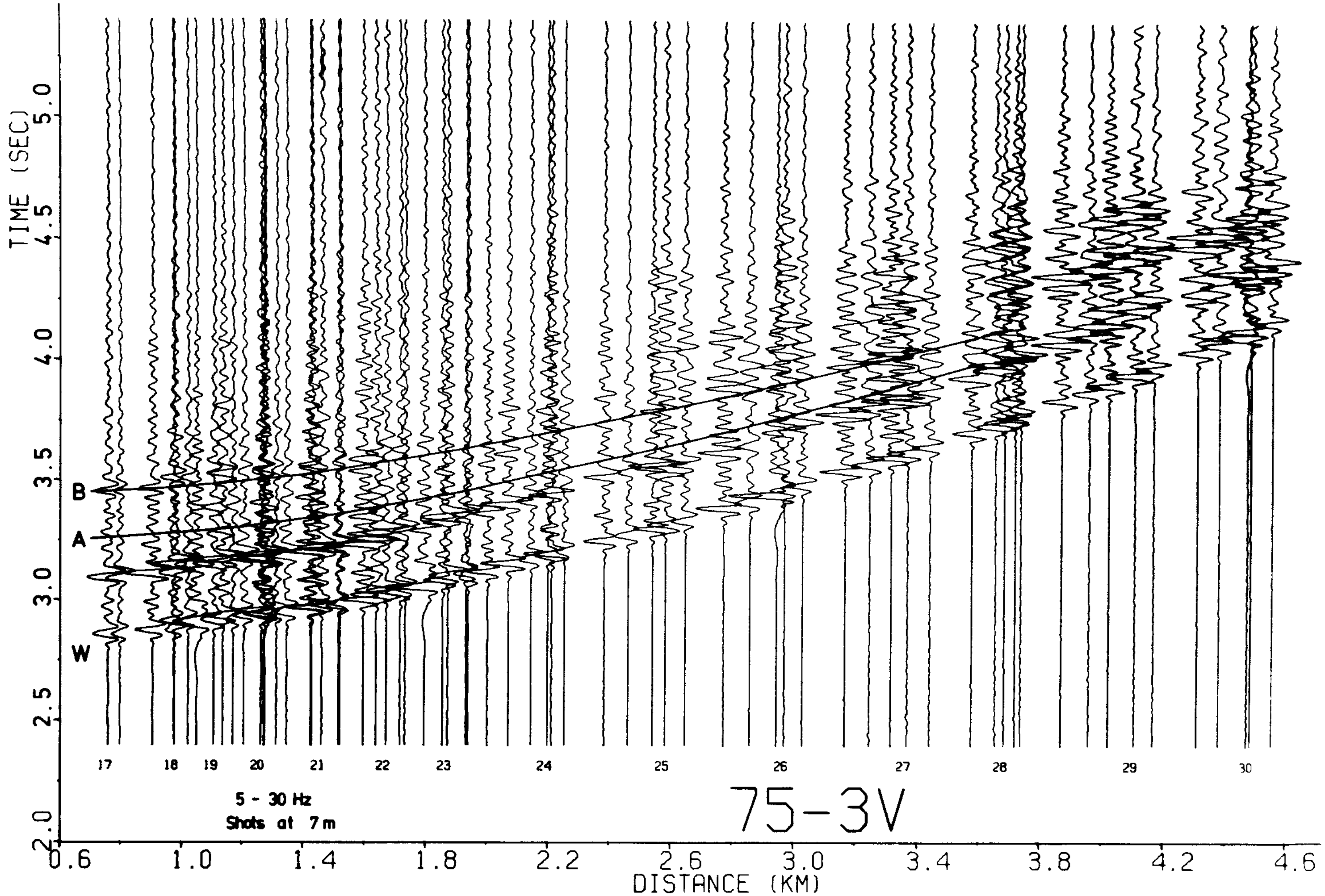

Fig. 3.2 Record section for reflection profile 75-3V.

2) Profiles 75-2, 75-2R, 75-3 and 75-3R

Profiles 75-2, 75-2R, 75-3 and 75-3R were each shot twice, first with shots at 7 m depth and then again with shots at 45 m. None were shot as split-dip profiles. Comparison of the record sections for the two shot depths for profile 75-2R reveals significant differences (see Figs. 3.3 & 3.4). The major difference is caused by the bubble pulse period, which is much less for the deeper shots than for the shallow shots. For identifying primary arrivals it was found that the shallow shot profiles were much better because the bubble pulse arrivals were more spread out in time and were relatively easy to identify. The bubble pulse period for the deeper shots is close to the dominant wave period of .06 - .10 s which made identifying individual bubble arrivals impossible and gave the records a much more reverberatory nature. The initial reason for placing the shots at 45 m was to direct more energy into the ocean bottom, but from comparison of the records it is not obvious that this resulted. The record sections for profiles 75-2, 75-3 and 75-3R are shown in Figs. 3.5, 3.6 and 3.7 respectively.

Another problem which caused some obscuring of the records was a result of the recording procedure when collecting data over a dipping reflector. In contrast to normal land seismic operations, marine seismic profiling requires a stationary array of receivers and a varying sequence of shot positions. If the horizon is dipping in the direction of the shooting ship the overall profile is considered to be a down-dip profile and the apparent velocity

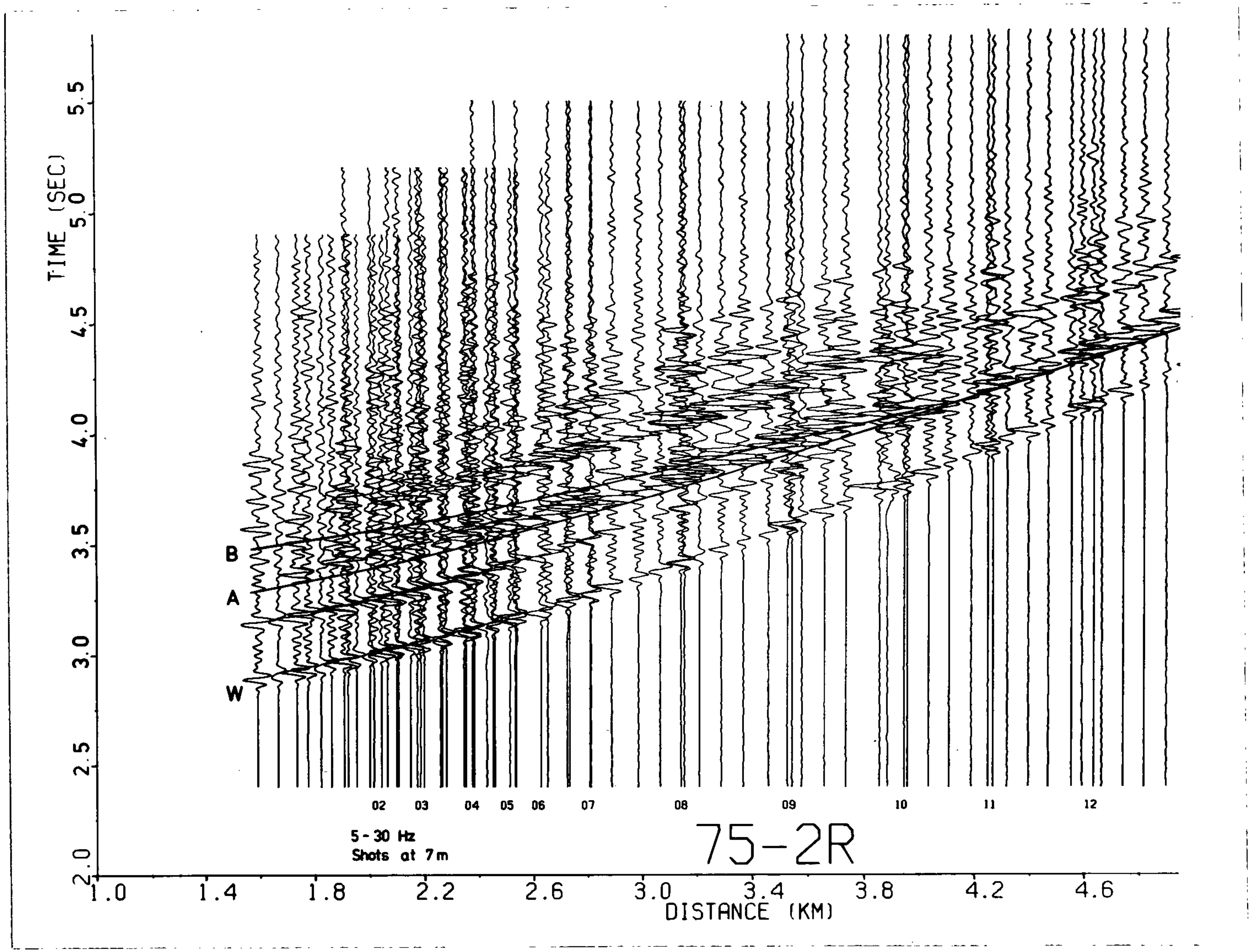

Fig. 3.3 Record section for reflection profile 75-2R (western end of line) with shots at 7 m depth.

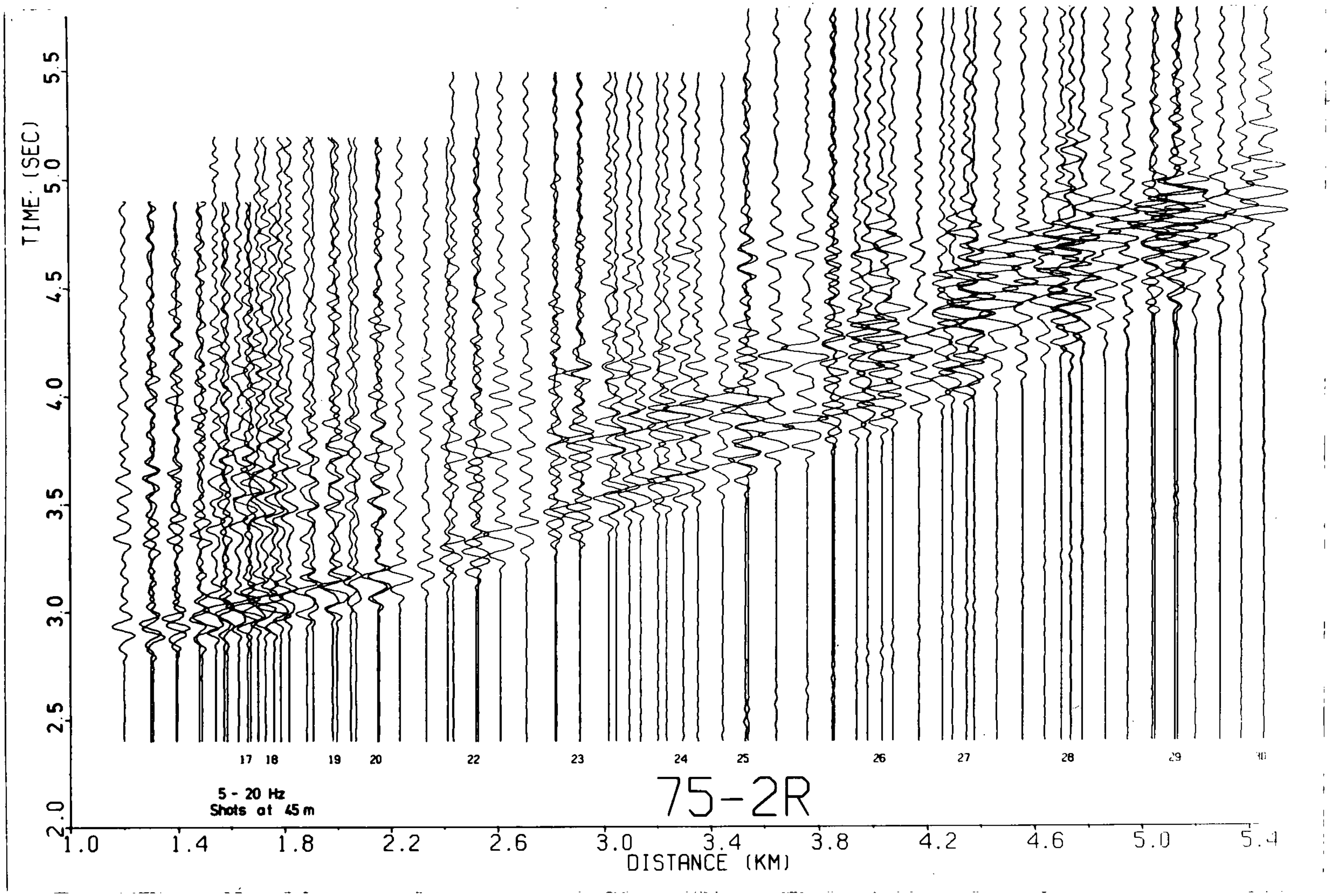

Fig. 3.4 Record section for reflection profile 75-2R with shots at 45 m depth.

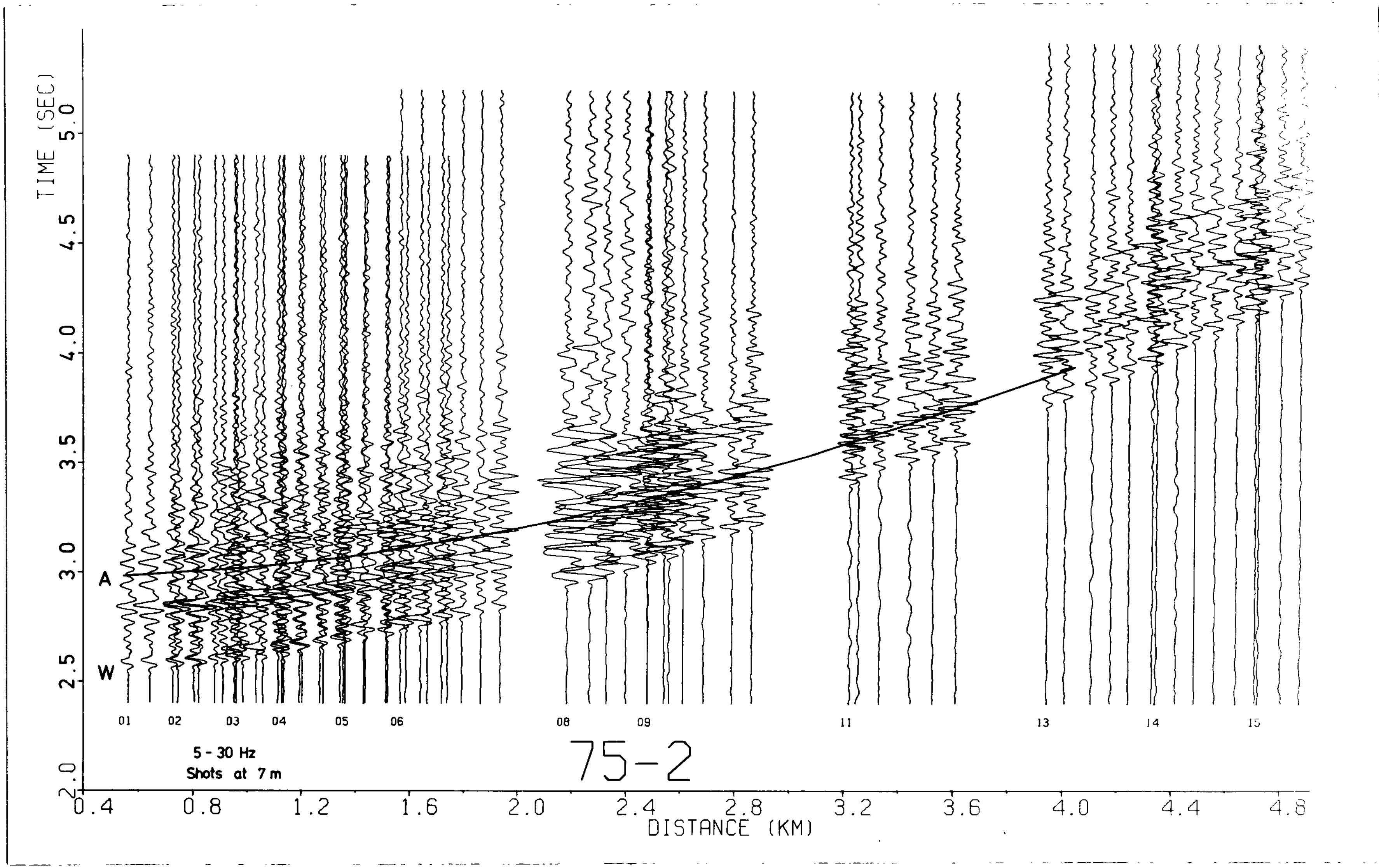

Fig. 3.5 Record section for reflection profile 75-2 (eastern end of line).

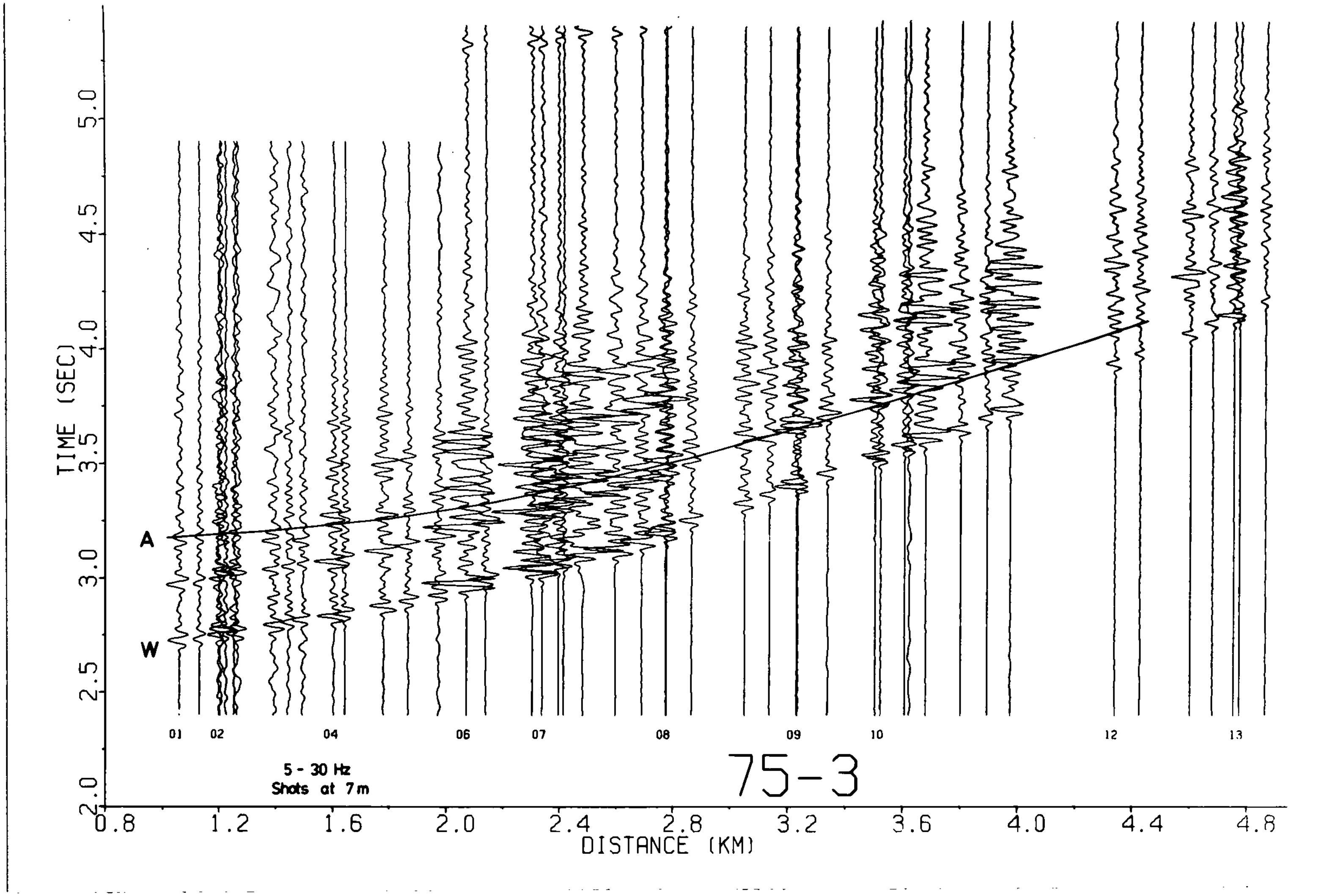

Fig. 3.6 Record section for reflection profile 75-3 (eastern end of line).

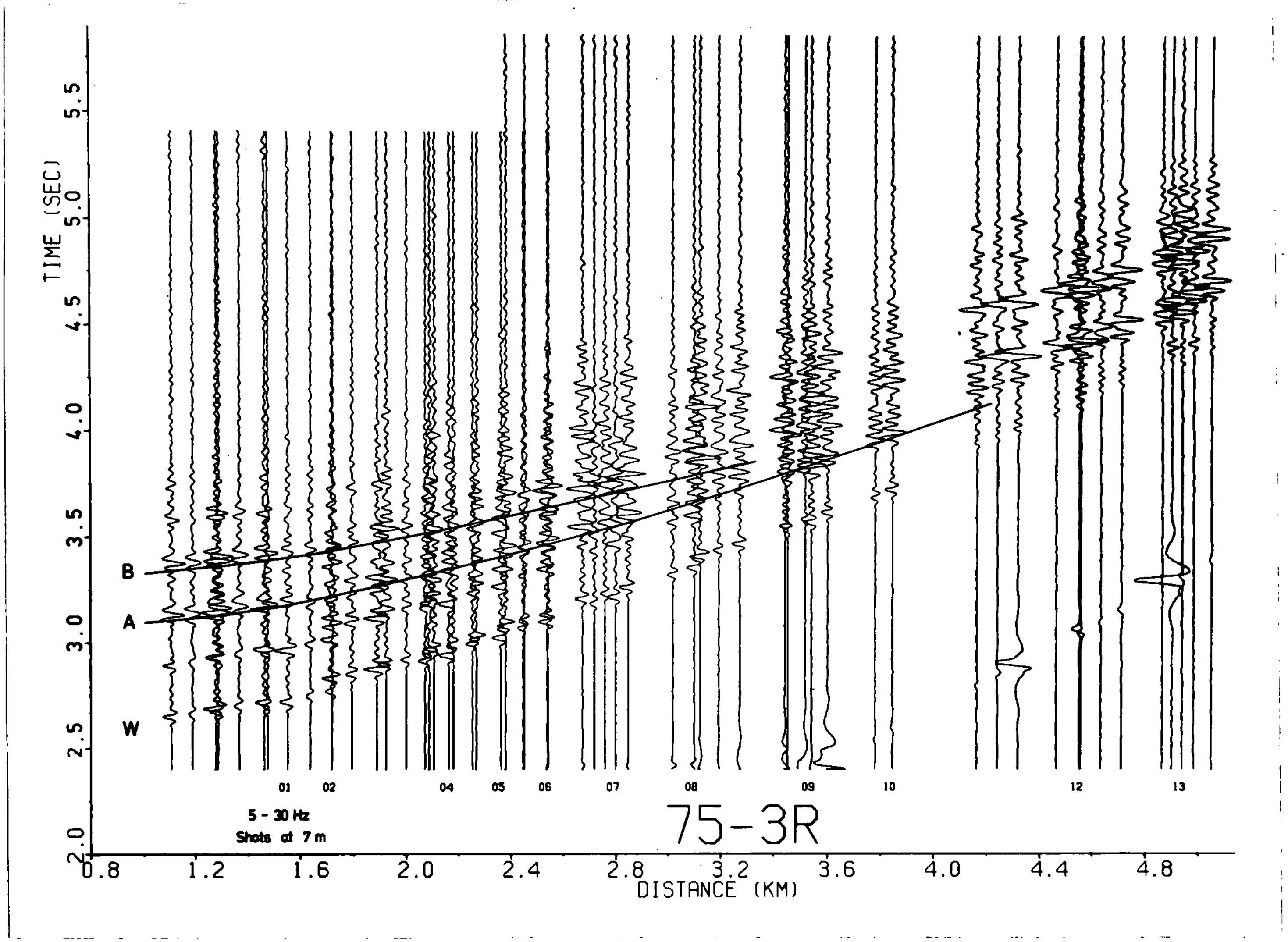

Fig. 3.7 Record section for reflection profile 75-3R (western end of line).

across the record section is lower than if the reflector is horizontal. However, for a single shot the energy is traveling up-dip to the receivers and the apparent velocity across the array of six hydrophones is higher than for a horizontal reflector. This results in arrivals not being smoothly continuous across the section but appearing as a series of short segments offset from each other by an amount which depends on the degree of reflector dip. This problem occurred to some extent in each of profiles 75-2, 75-2R, 75-3 and 75-3R, which the C.S.P. records show as having dipping sea floor, and made the correlating of coherent phases very difficult in places.

It was possible to identify only one or two primary reflections from the record sections of these four profiles. This also is consistent with the C.S.P. records and petroleum industry reflection data which show no coherent reflections beyond these arrival times for similar regions. Any deeper crustal reflections, if present, have low amplitudes and are obscured by noise and bubble pulse reverberations.

As mentioned in the previous section these profiles are not split-dip and must be analyzed using equation 3.7. Examination of the C.S.P. records shows that for profiles 75-2R and 75-3R the basement dip is about 5° towards the east, whereas for profiles 75-2 and 75-3, the dip is not clear. Using the C.S.P.-determined values gives a sub-bottom layer 0.8 km thick with velocity 2.45 km/s for 75-2R and 0.65 km thick with velocity 2.42 km/s for 75-3R. Several different dips were tried with 75-2 and 75-3. Varying the dip from 2°

Table II Reflection interpretation results for profiles 75-2, 75-2R, 75-3 & 75-3R. Three sets of possible results are shown for the bottom layer of each profile since there is an ambiguity between velocity, thickness and dip.

Profile	Layer	Velocity (km/s)	Thickness (km)	Dip (deg)
75-2R	W	1.49	1.80	0.0
	A	2.45	.80	5.0
	B	3.01	.30	3.0
	B	3.47	.35	4.0
	B	3.90	.39	5.0
75-3R	W	1.49	1.80	0.0
	A	2.42	.65	5.0
	B	2.66	.34	3.0
	B	3.09	.40	4.0
	B	3.52	.45	5.0
75-2	W	1.49	1.77	0.0
	A	2.42	.59	2.0
	A	2.85	.65	4.0
	A	3.24	.71	6.0
75-3	W	1.49	1.75	0.0
	A	2.51	.78	2.0
	A	2.81	.84	4.0
	A	3.11	.91	6.0

to 6° resulted in velocities varying from 2.42 km/s to 3.24 km/s with an average thickness of 0.65 km for profile 75-2 and velocities varying from 2.51 km/s to 3.11 km/s with an average thickness of 0.85 km for profile 75-3.

For profiles 75-2R and 75-3R it was possible to arrive at velocities and thicknesses for a 2nd sub-bottom layer for a range of possible dips. These values plus a summary of the results of this section are shown in Table II.

4. REFRACTION ANALYSIS

4.1 THE REFRACTION DATA SET

The reduced record sections for refraction profiles 75-2, 75-2R, 75-3 and 75-3R are shown in Figs. 4.1, 4.2, 4.3 and 4.4, respectively. A reducing velocity of 6.0 km/s has been used and all traces have been filtered from 5 to 20 hz. Each set of 6 traces (or less if particular channels were defective) is labeled with its shot number, which is also shown on the appropriate C.S.P. record (Fig. 1.3 or 1.4). As described previously, topography has been corrected to a constant water depth of 2.0 km using a velocity of 1.49 km/s for the water layer and 2.0 km/s for the sub-bottom material. The 2.0 km/s for the sub-bottom is representative of shallow sediments in this area as determined from the results of Chapter 3. For shots over the shallower waters of the continental shelf and slope, 2.0 km/s is probably too low. This problem was encountered for the last few shots of profiles 75-2R and 75-3R.

First arrival picks were made from the same plots as the D.W.W. arrivals (Fig. 2.1) and are indicated on the record sections by solid triangles. Weaker and more emergent arrivals are indicated by slightly smaller triangles. All four record sections show extended wavetrains after the first arrival breaks but few coherent secondary arrival branches. The first water bottom multiple at the shooting ship comes in beyond the end of the traces for most shots but is visible for

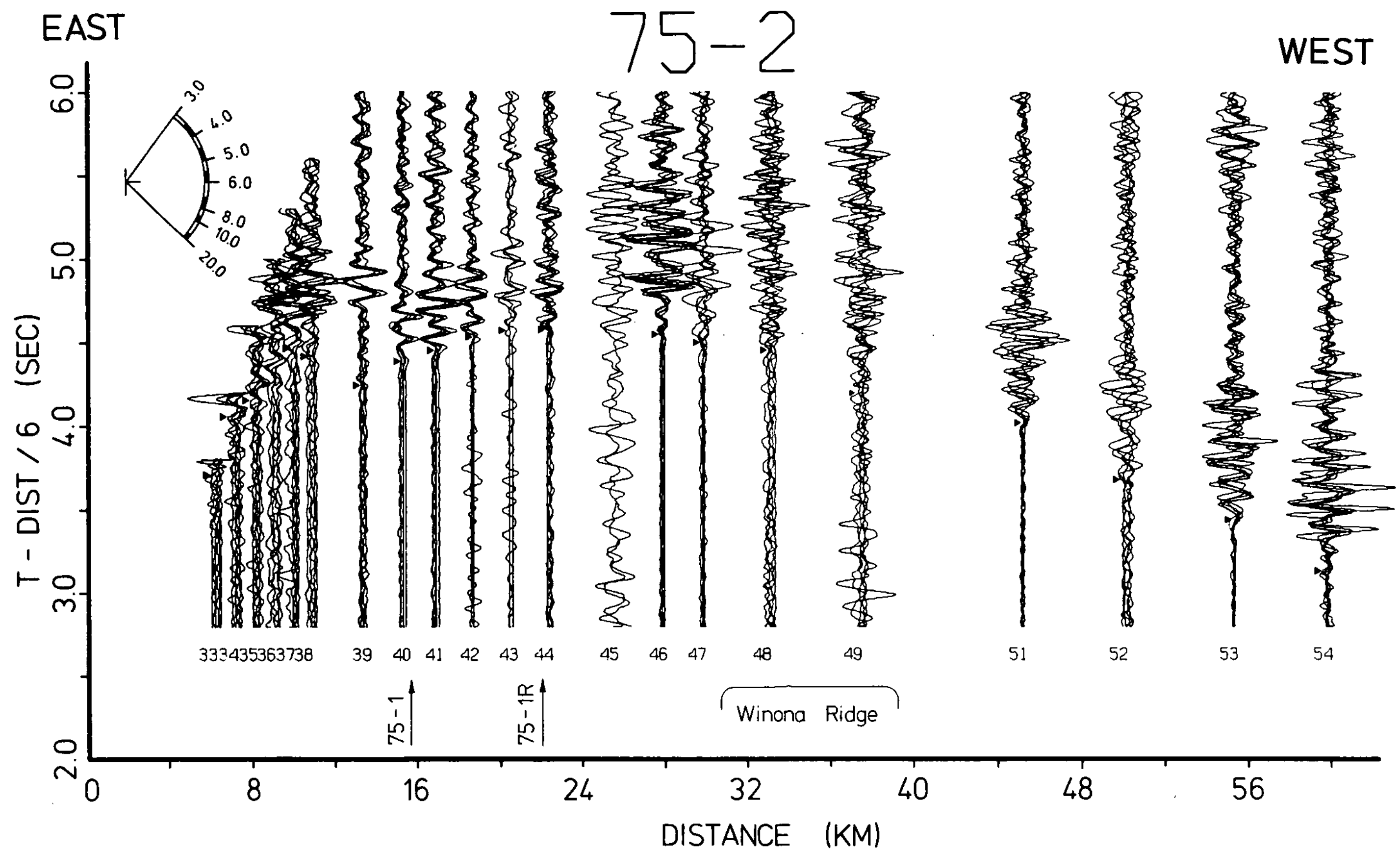

Fig. 4.1 Reduced record section for refraction profile 75-2. The solid triangles indicate first arrival picks; the smaller ones correspond to more emergent arrivals. All traces have been filtered from 5 to 20 hz. Each set of six traces is labeled with its corresponding shot number. Amplitude correction with distance is r².

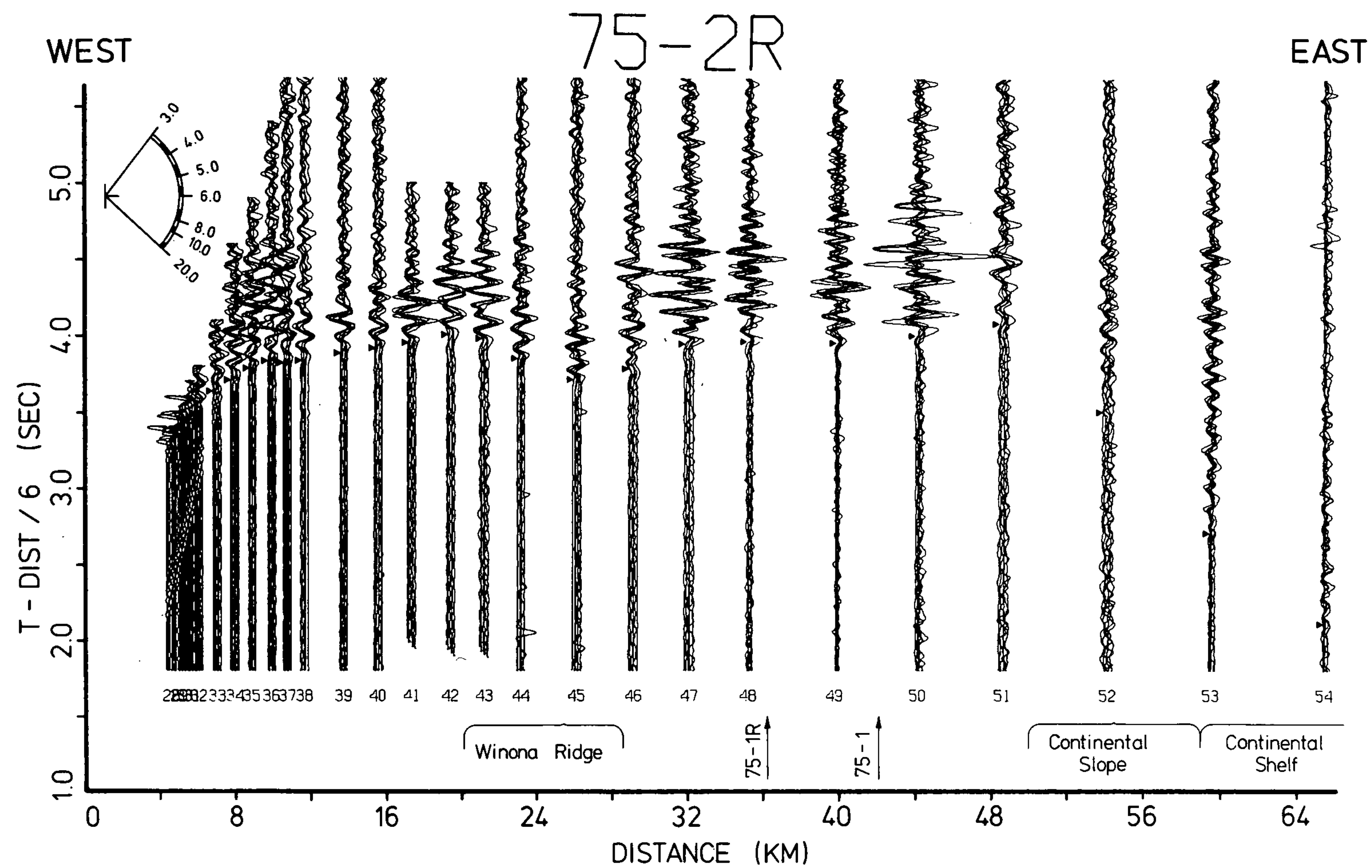

Fig. 4.2 Reduced record section for refraction profile 75-2R.

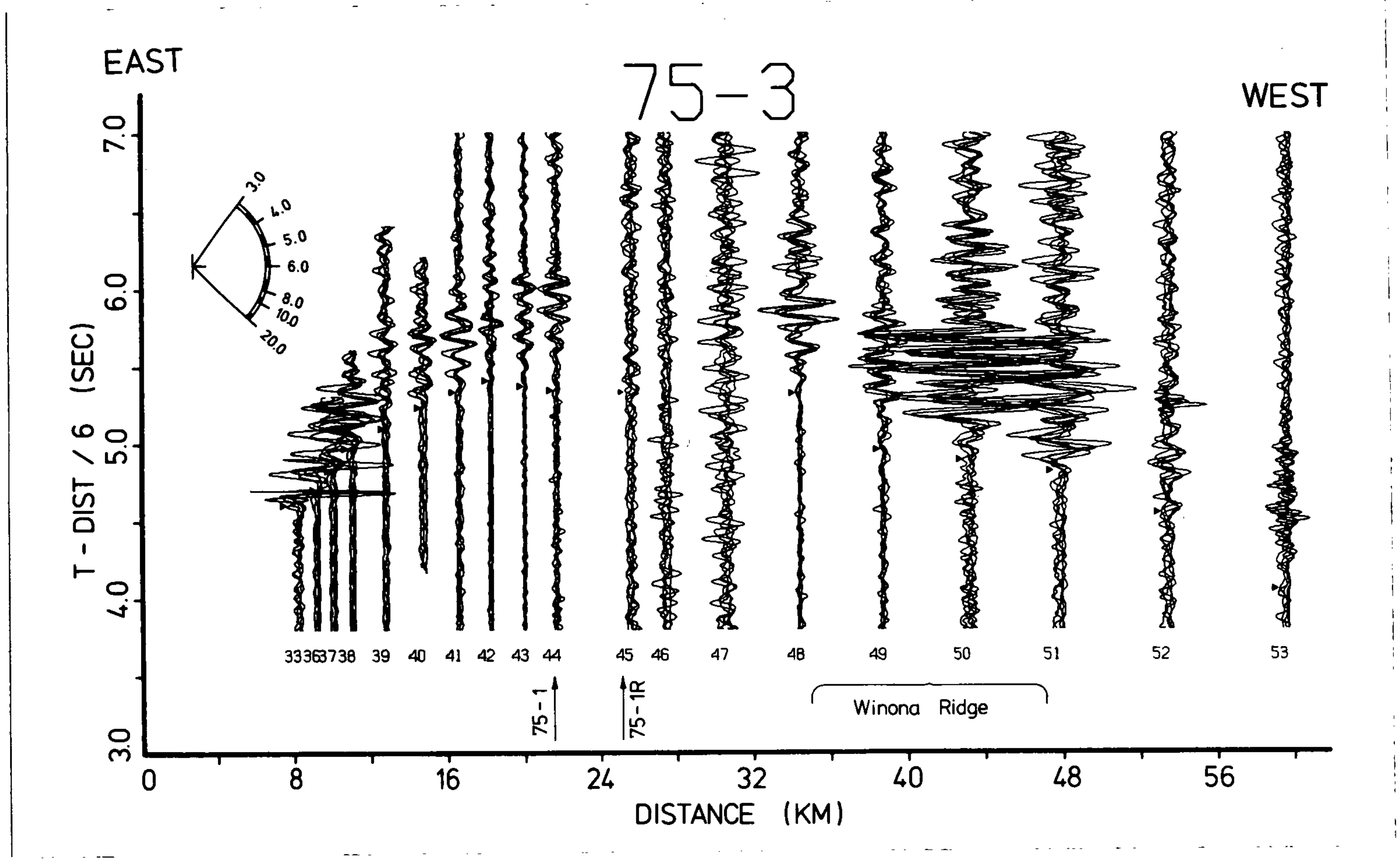

Fig. 4.3 Reduced record section for refraction profile 75-3.

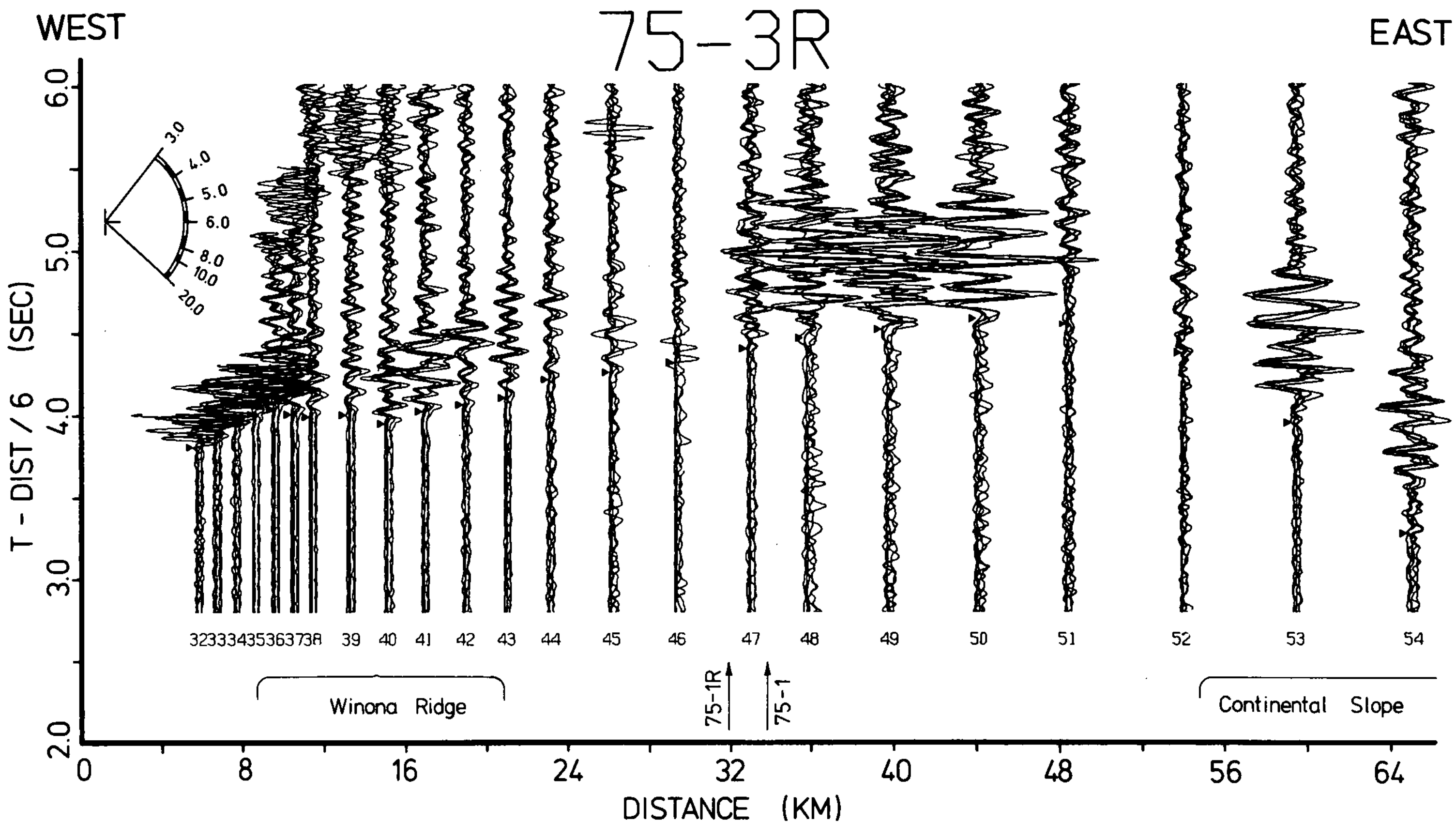

Fig. 4.4 Reduced record section for refraction profile 75-3R.

some of the distant shots, for example at 5.6 s for shot 54 of profile 75-3R.

Close examination of the record sections reveals many unusual characteristics. Some of these are consistent with the C.S.P. records while others are not. On profile 75-2 (Fig. 4.1) a 0.2 s travel time advance between shots 38 and 39 corresponds to a fault at the foot of the continental slope, clearly visible on C.S.P. record 75-2. A 0.1 s advance at shot 49 corresponds to rays traveling up through Winona Ridge and possibly indicates higher velocity material beneath the ridge than on either side. The furthest first arrival branch, starting at 44 km has an apparent velocity of 9.8 km/s which is consistent with upper mantle head waves traveling up dip. This would be expected if the oceanic crust is dipping towards or beneath the continental crust. The amplitudes for this profile are relatively uniform although increases are observed on shot 51 and later shots.

The most striking feature of profile 75-2R (Fig. 4.2) is the 0.25 s travel time advance centered at shot 45. This corresponds precisely with Winona Ridge and is a certain indication of higher velocity material beneath the ridge than on either side. The furthest first arrival branch, starting at 48 km has a very high apparent velocity of 20 km/s. This could be partly due to the low velocity of 2.0 km/s used for the large topographic correction necessary. Using a velocity of 6.0 km/s for the correction results in an apparent velocity of 10.1 km/s for the branch. Since the proper topographic correction velocity must be between these two extremes there is a strong implication that the interface from which these arrivals were critically refracted must be dipping towards the west since the refracting velocity is not likely to be much greater than 8.0 km/s. Amplitudes for this profile are relatively uniform out to about 30 km. They increase between 32 and 45 km beyond which they decrease significantly to the end of the profile.

On profile 75-3 (Fig. 4.3) a slight travel time advance at shot 44 could correspond to either a fault or a positive horizontal velocity gradient. The influence of Winona Ridge is seen on shots 49 and 50 as a 0.2 s travel time advance. The furthest first arrival branch, starting at 52 km has an apparent velocity of 12.0 km/s, consistent with an eastward dipping crust. Amplitudes for this profile show considerable variation, with weak arrivals from 22 to 25 km followed by no detectable arrivals out to 32 km. They then increase to very strong at 43 km and fade gradually to the end of the profile. This wide variation in amplitudes could be the result of focusing of rays by Winona Ridge.

Profile 75-3R (Fig. 4.4) has a 0.15 s travel time advance over Winona Ridge and a final first arrival branch starting at 58 km with an apparent velocity of 20 km/s. As for profile 75-2R the topographic corrections are probably too small. Using 6.0 km/s for the correction results in an apparent velocity of greater than 10.0 km/s, again indicating a westward dipping interface. Large amplitudes are observed from 32 to 46 km and at 59 km, and very weak arrivals from 23 to 30 km and from 48 to 54 km.

In general the sets of profiles shot in the same direction are consistent with one another. This is particularly true for the effect of Winona Ridge and the apparent velocities of the furthest first arrival branches. For profiles 75-2 and 75-3 an eastward dipping deep interface is indicated for the west side of the basin while for 75-2R and 75-3R a westward dipping deep interface is indicated for the east side of the basin.

4.2 METHODS OF ANALYSIS

Several methods exist for interpreting seismic refraction data. The best one to use for a specific case depends on the profiling method and the physical characteristics of the area of interest. Those techniques most applicable to this type of study are first arrival analysis, synthetic seismogram computation and ray tracing.

1) First Arrival Analysis

This method assumes a model which consists of discrete, constant velocity layers separated by plane, arbitrarily dipping interfaces. There can be no lateral variations normal to the profile line. Mota (1954) derives equations for dip, velocity, depth and thickness for the n-layer case. The profile must be shot in both the forward and reverse directions. Since only the arrival times of the first refraction energy are used, much information, such as relative amplitudes and secondary arrivals, is neglected.

2) Synthetic Seismogram Computation

A method which makes use of the entire suite of seismic data is the computation of synthetic seismograms. Techniques devised to date, such as "disc-ray theory" (DRT) by Wiggins (1976), impose the restriction of lateral homogeneity. For DRT a starting model is often derived from first arrival analysis. The first arrival velocity-depth curve is used to generate a ray parameter vs. distance (P-X) curve which in turn is used to generate a travel time curve, a velocity-depth curve and a set of synthetic seismograms. The travel times and amplitudes are compared with the real data and if necessary, the P-X curve is altered and the process repeated. This method was used by Lynch (1977) to analyze the set of reversed profiles 75-1 and 75-1R taken along the eastern portion of Winona Basin, parallel to the continental margin (see Fig. 1.2). Lateral variations along these lines are most likely small, justifying the assumption of lateral homogeneity.

3) Ray tracing

A method which imposes a minimum in model restrictions is ray tracing. The model can consist of any number of arbitrarily shaped zones of any velocity or velocity gradient. Rays are sent out from the origin at equal angular increments and "traced" through the model by applying Snell's Law at the interfaces and following the appropriate trajectory through the gradient zones. The travel time for each ray to return to the surface is computed and plotted on a time-distance curve for comparison with the real data. An indication of relative amplitudes can be obtained by observing on a ray plot the spacing of arrivals at the surface; many arrivals in a short distance correspond to increased amplitudes. Choosing a starting model for a complex area can be very difficult and requires consideration of first arrival information, surface geology, regional tectonics and any information which can be obtained from other geophysical methods.

Ray tracing has been used by Clee et al (1974) as an aid in the interpretation of a detailed reflection-refraction study near Yellowknife, Northwest Territories, and by Miller and Gebrande (1976) and Grubbe (1976) in refraction studies of Central Europe.

As demonstrated in Section 4.1, close examination of the record sections in conjunction with the C.S.P. records indicates strong lateral variations in both sets of profiles. The travel time advance observed consistently over Winona Ridge on all profiles indicates significantly higher velocities beneath the ridge than on either side. A major fault is indicated by profile 75-2 and possibly by profile 75-3. The high apparent velocities at the ends of all four refraction lines indicate interfaces deep within the crust which dip from both sides of the basin towards the center. These observations immediately rule out synthetic seismograms as an interpretation technique for these profiles. The lateral inhomogeneities are much too severe to attempt to use a laterally homogeneous model. Furthermore, first arrival analysis cannot be used for the overall sections because there appear to be interfaces which are either not plane, or do not extend over the entire profile, as indicated by the high apparent velocities at the ends of the refraction lines. This means that the forward and reverse lines do not have easily identifiable corresponding first arrival branches.

This leaves ray tracing as the only acceptable interpretation technique. Information for selecting a starting model can be obtained from refraction profiles 75-1 and 75-1R (Lynch, 1977), reflection results from Chapter 3 and unreversed first arrival analysis of the start of each refraction line. The first two sources provide well established results; however, the first arrival analysis requires assumptions concerning apparent velocities of hypothetical reverse profiles which will give reasonable layer thicknesses and dips.

4.3 DESCRIPTION OF RAY TRACING PROGRAM

Having decided upon ray tracing as the most suitable method of interpretation of the refraction data it was necessary to obtain a computer program to perform the actual tracing of the rays and produce travel time curves and ray plots. The type of program needed was one which could handle several layers with arbitrarily shaped polygonal boundaries and any desired velocity or linear velocity gradient. Since no existing programs in the department met these specific requirements a decision was made to develop the program here.

The completed program, written by Ken Whittall, accepts several polygonal shaped layers as input. The velocity in a layer is defined as being constant along its top boundary and varying linearly with depth normal to this boundary. Rays leave the origin at equal angular increments over a specified range of angles. Since all layers have non-zero linear gradients, all ray paths are circular arcs with radius and center depending on the velocity and gradient. If a ray intersects another boundary, Snell's law is applied using the velocities on either side of the interface, and a new circular trajectory is computed from the new gradient. The travel time for each circular segment is calculated and when the ray eventually returns to the surface the total travel time is determined by summation and plotted against its arrival distance. Constant velocity layers are closely approximated by specifying a very small gradient.

The generation of head waves is not predicted by ray theory and requires the theory of wave propagation for a full description. For this reason, pseudo head wave arrivals are generated artificially by the ray tracing program. If a ray intersects a boundary within some specified angle of the critical angle, critically refracted rays are generated at regular intervals along the boundary to simulate the upward traveling energy associated with true head wave arrivals.

The ray tracing program produces a computer plot of the model with ray paths superimposed and a plot of travel times vs. distance for all ray arrivals. On the travel time plots, reflected rays are identified by crosses and head waves by

X's. The travel time plot can be reduced to any velocity and plotted at any scale for easy comparison with record sections of real data. Once a good fit has been made to first arrival travel times the concentration of arrivals on the travel time and ray plots can be used as a qualitative measure of amplitudes. Fitting first arrivals for a single profile certainly does not guarantee a unique model; however, if the travel times and relative amplitudes can be satisfied for both a forward and reverse profile, then the reliability of the model is improved significantly, although it is still not unique.

4.4 APPLICATION OF RAY TRACING

In order to apply the ray tracing technique to the interpretation of a refraction profile, a starting model must first be chosen. A ray plot and travel time curve are then generated for both the forward and reverse directions and compared with the real data. If necessary, alterations are made to the model until the travel time fit is acceptable and the relative amplitudes agree qualitatively.

Profiles 75-3 and 75-3R:

To illustrate the detailed application of the ray tracing technique the set of reversed profiles 75-3 and 75-3R will be used.

a) The Starting Model

The starting model for profile 75-3 is shown in Fig. 4.5.

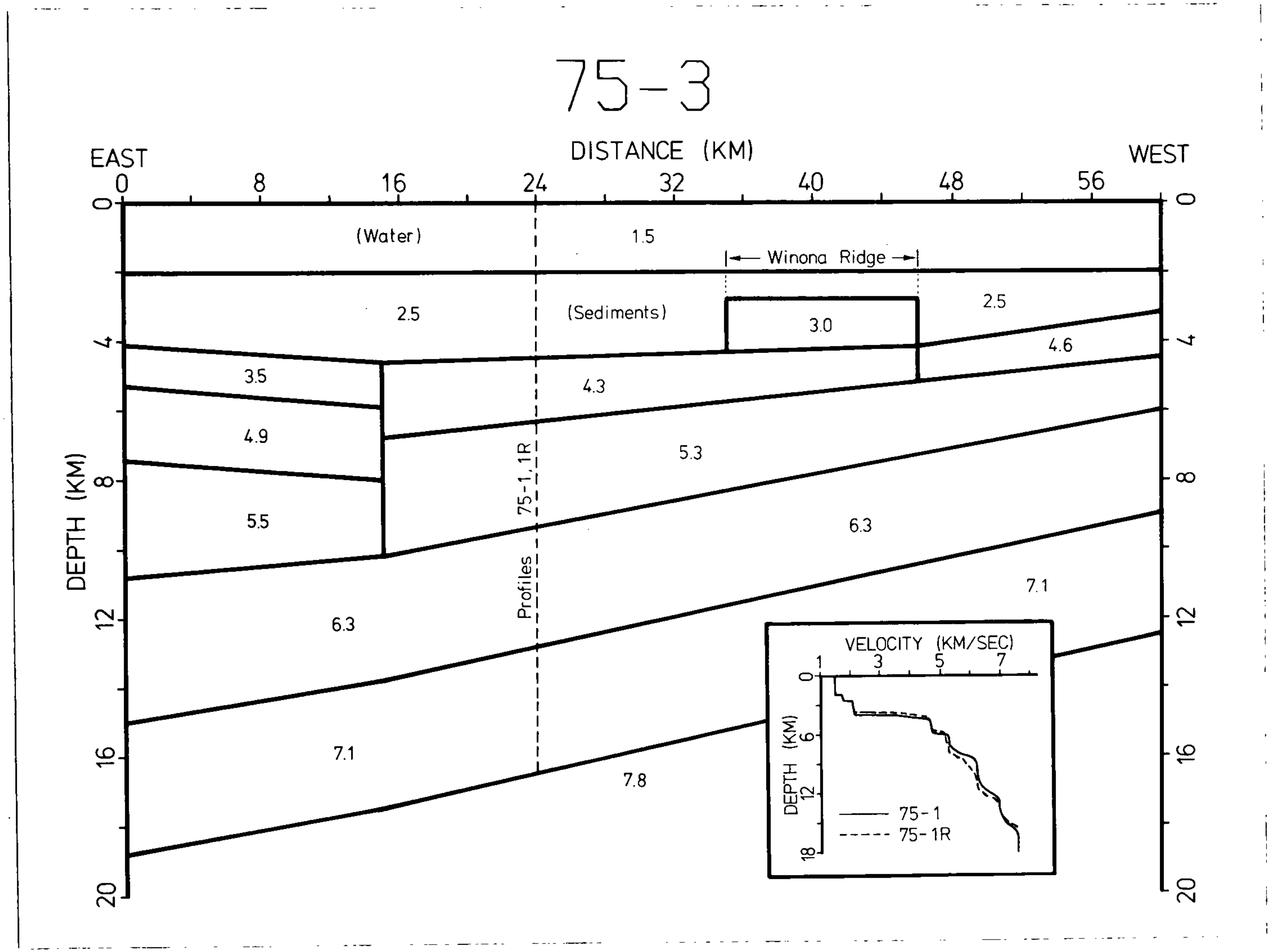

Fig. 4.5 Starting model for ray tracing of profile 75-3. The inset shows the final velocity-depth curves for refraction profiles 75-1 and 75-1R arrived at by Lynch (1977) using DRT synthetic seismograms. These were used as a constraint for the cross-basin profiles. Numbers within model blocks are velocities in km/s.

The results of the first arrival interpretation of the set of reversed profiles 75-1 and 75-1R (Lynch, 1977) are represented by the vertical line through 24 km, and provide the only set of constraints that extend throughout the entire crust. The inset shows Lynch's final velocity-depth curves for these profiles determined from a traveltime and amplitude interpretation using DRT synthetic seismograms.

The top few layers on the east end of the section were obtained by performing a first arrival analysis on the first few travel time branches of profile 75-3, with an assumption of plane, continuous layers over the first 10 to 20 km. A computer program, based on the equations for dip, velocity, depth and thickness for several plane layers (Mota, 1954) was used to generate sets of layers with different velocities, thicknesses and dips, all of which satisfy the travel times for the beginning of the profile. A unique set of layers cannot be determined because the profile segments are effectively not reversed. The arrivals from these layers on the reverse profile 75-3R, if present at all, are secondary and virtually impossible to identify. The number of possibilities can be reduced, however, by applying certain restrictions to the velocities or dips of the layers. For example, assuming an average velocity of 2.5 km/s for the first sub-bottom layer is consistent with the reflection results of Chapter 3. Choosing a velocity of 4.3 km/s for the second layer is consistent with profile 75-1 but requires a dip of 11° to the west for the first sub-bottom interface and 4° to the east for the second. Consequently, a velocity of

3.5 km/s was chosen as the starting value for this layer because it resulted in both interfaces dipping to the west. Applying the same procedure to profile 75-3R resulted in layers with similar velocities to those of 75-1, all dipping towards the east. Since this is consistent with the C.S.P. record (Fig. 1.4) and a crust thickening towards the continent, these layers were used for the west side of the starting model for profile 75-3.

As mentioned in Section 4.2, a travel time advance is observed on all profiles for shots over Winona Ridge. This is represented on the starting model by the block of material with velocity 3.0 km/s. Beyond this there is no further direct seismic information which can be used to complete the starting model, particularly for the deeper layers. The choice of these layers as shown in Fig. 4.5 was made simply by having them dipping towards the continent and intersecting the 75-1 layers. This is consistent with subduction and whether correct or not, it will be sufficient for a starting model.

Since profile 75-3R was not shot directly over 75-3 (see Fig. 1.2), its starting model is slightly different than for 75-3. This is necessary to reflect the differences in profile length and topography. The same situation also applies to 75-2 and 75-2R.

In summary, the main constraints on the models are i) the results of profile 75-1, 1R, ii) the profiles being approximately reversed, iii) the C.S.P. records, iv) current views on plate tectonics and v) the crust thickening from typical oceanic crust to a thicker continental crust (up to 30 km) from Winona Basin to the continental shelf. For any model to be acceptable it must be consistent with these constraints.

b) Testing the Models

The ray plots and reduced travel time curves for ray tracing on the starting models for profiles 75-3 and 75-3R are shown in Figs. 4.6 and 4.7. The circles connected by dashed lines on the travel time curves represent the first arrival times taken from the record sections (Figs. 4.3 & 4.4). For profile 75-3 the agreement is quite good over most of the profile, the arrivals being 250 ms late at 24 km and 100 ms late from 50 km to 60 km. For 75-3R however, the agreement is good only at the start, which is expected because of the way in which the initial model was constructed, and poor over the remainder of the profile. To make the arrivals earlier over Winona Ridge (11 to 21 km) the ridge velocity was increased to 3.7 km/s, more representative of consolidated sediments. In order to greatly increase the apparent velocity of the first arrivals beyond 50 km some of the layers against the east side of the basin were made to dip towards the west. These changes greatly improved the 75-3R fit without seriously affecting the reasonably good fit of the 75-3 model. Many subsequent trials were made, with the travel time fits gradually improving at each step.

c) The Final Models

Eventually, models were found which satisfied both 75-3 and 75-3R travel times very well. These models, with rays superimposed, are shown in Figs. 4.8 and 4.9 along with their

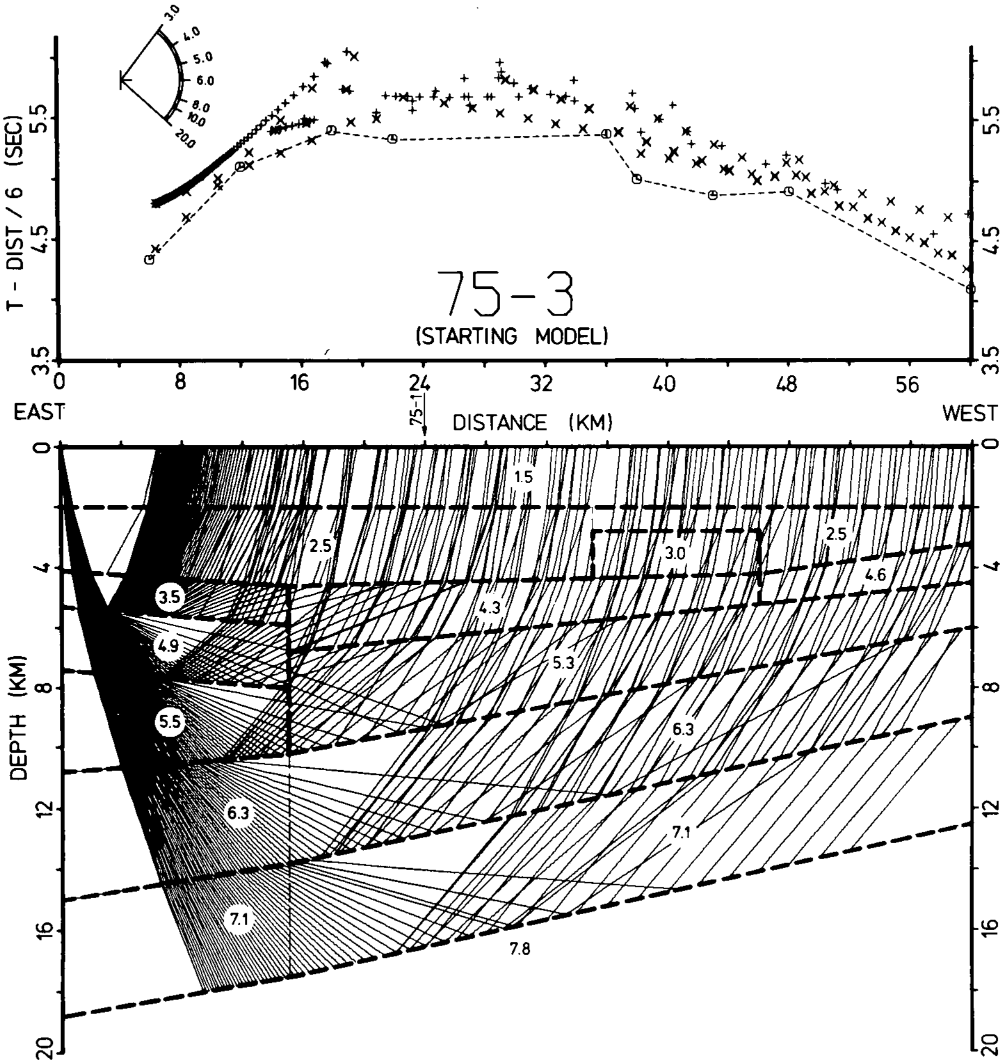

Fig. 4.6 Ray plot and travel time curve for 75-3 starting model. The dashed line on the travel time curve represents the first arrival picks taken from the record section. Numbers within blocks outlined by heavy dashed lines are velocities in km/s.

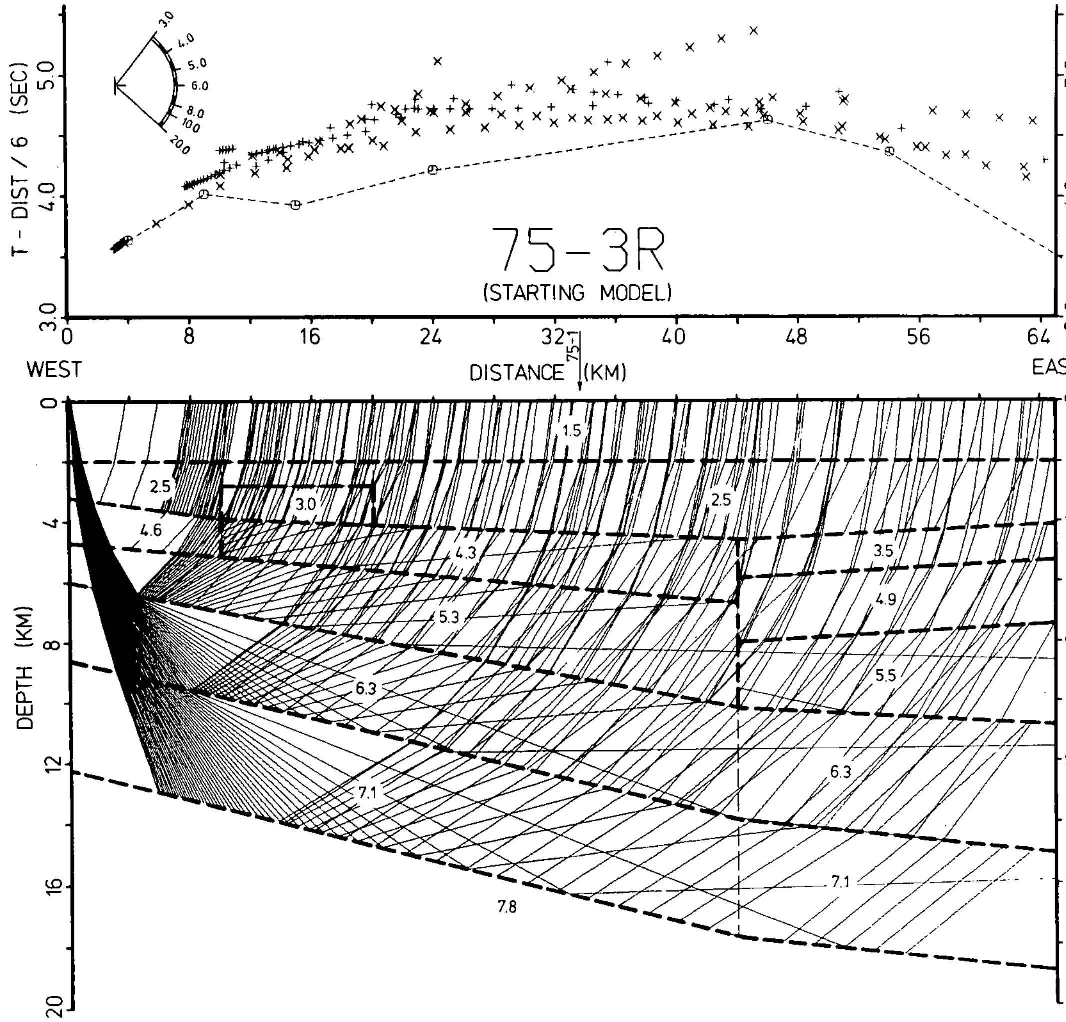

Fig. 4.7 Ray plot and travel time curve for 75-3R starting model. The model is identical to 75-3 except for differences arising from the two profiles not being exactly coincident. Note that the model is reversed, west being on the left, compared with Fig. 4.6. Numbers within blocks outlined by heavy dashed lines are velocities in km/s.

respective travel time curves. By identifying the boundaries from which all head wave branches were refracted, it was found that head waves from the bottom interface never appear alone as first arrivals, although on the final branch of each profile (beyond 48 km) these arrivals plus arrivals from the next higher interface come in almost simultaneously as first arrivals. For this reason the bottom interface is shown with question marks since the first arrival travel times could be satisfied without it.

Examination of the model travel time curve for profile 75-3 shows that the first arrival travel time fit is very good. The slight advance observed at 22 km was modeled by placing the 3.5 km/s and the 4.3 km/s layers together, simulating a horizontal velocity gradient in the vicinity of their boundary. This same effect could have been produced by a fault in the sediments, but would have required a change in the dips and velocities of these layers which would have made it very difficult to fit the first arrival branches satisfactorily. The early arrivals from 36 to 48 km corresponding to paths through Winona Ridge agree very well with the observed travel times. The same results could have been obtained by decreasing both the thickness of the ridge layer and its velocity. This implies an upper limit of approximately 3.7 km/s for the ridge velocity.

As for profile 75-3, the model travel time curve for profile 75-3R shows a very good fit to the observed first arrivals. The travel time advance over Winona Ridge is well modeled and the high apparent velocity of the final branch has

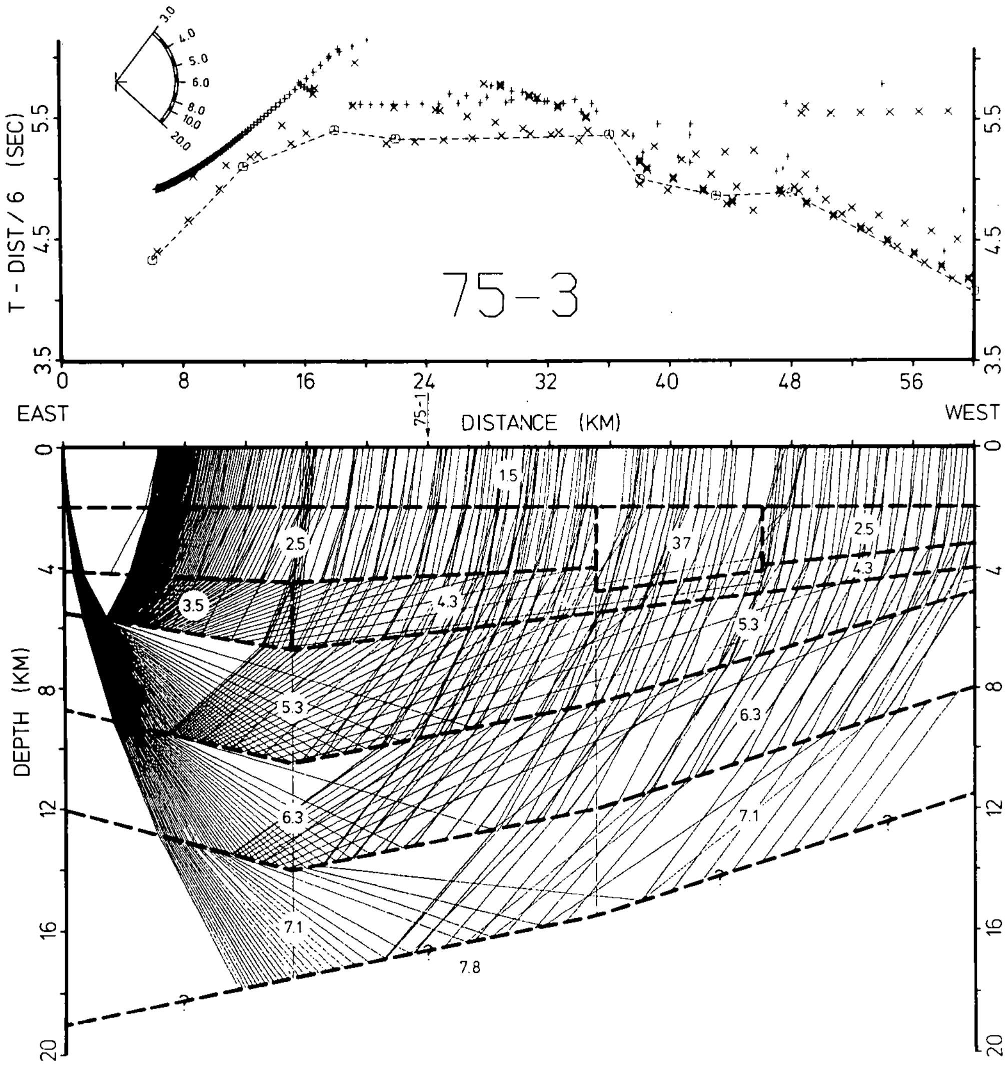

Fig. 4.8 Ray plot and travel time curve for 75-3 final model. The question marks on the bottom interface indicate that the first arrival travel times could be satisfied without arrivals from this boundary; therefore its position is not definite. Numbers within blocks outlined by heavy dashed lines are velocities in km/s. Vertical exaggeration is 2X.

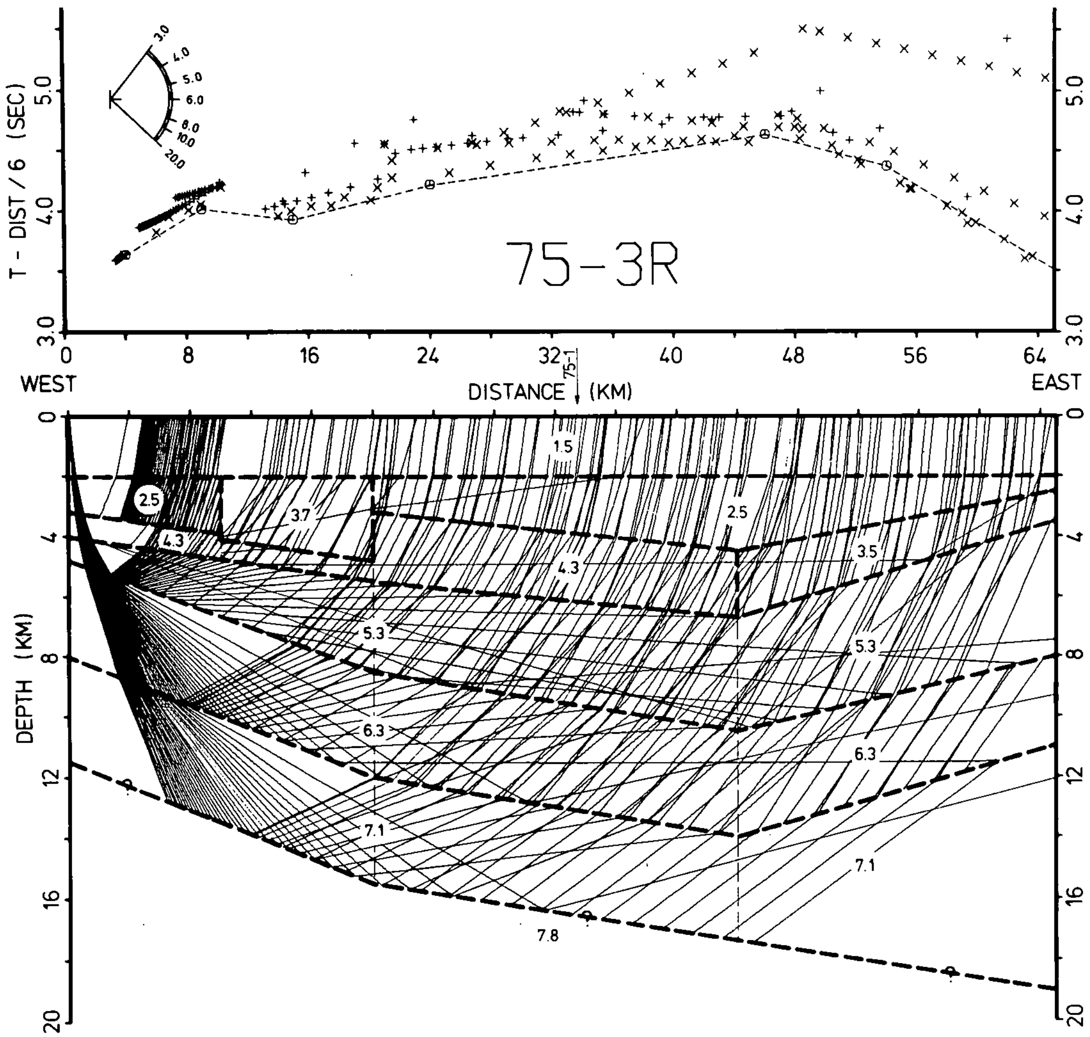

Fig. 4.9 Ray plot and travel time curve for 75-3R final model. The model is identical to 75-3 except for differences arising from the two profiles not being exactly coincident. Note that the model is reversed, west being on the left, compared with Fig. 4.8.

been achieved by the position of the westward dipping layers at the east side of the basin.

The model travel time curve for profile 75-3 shows a single head wave branch as the first arrival from 20 to 30 km. Being a pure head wave arrival, its amplitude is expected to be small in comparison with other reflected and refracted arrivals. This branch corresponds well with the weak first arrivals observed on the record section of 75-3 over the same range. About 0.3 s later on the model travel time curve a reflected and a refracted branch coincide to create the stronger secondary arrival which is observed on the record section. Similarly for profile 75-3R the weak arrivals from 22 to 32 km are generated by the head wave branch observed over this range on the model travel time curve and the large amplitudes from 34 to 48 km are generated by the large concentration of arrivals observed there.

Due to the difficulty in identifying secondary arrivals on the record sections, it was not possible to constrain the models by these arrivals. However, close comparison of the record sections with the ray travel time plots for 75-3 and 75-3R shows that some secondary arrivals can be tentatively identified. Elsewhere on the sections the amplitude agreement is generally good. Of course, it is not difficult to find areas of apparent contradiction on both sets of profiles. This is to be expected since the models consist of blocks of constant velocity material while in actual fact, with the exception of faults, the boundaries between layers are most likely zones of increased velocity gradient with very smooth lateral variations.

Profiles 75-2 and 75-2R:

The modeling procedure used for profiles 75-2 and 75-2R was almost identical to that used for 75-3 and 75-3R. The final models, with rays superimposed, are shown in Figs. 4.10 and 4.11 along with their respective travel time curves. The model travel time curves for profiles 75-2 and 75-2R agree very well with the observed first arrivals, with the exception of the last branch of 75-2R. The travel time advance observed between shots 38 and 39 for 75-2 was generated by a 0.7 km vertical fault in the sediment layer. As with profiles 75-3 and 75-3R a velocity of 3.7 km/s for the Winona Ridge layer generated the required travel time advance from 32 to 40 km on 75-2 and from 20 to 32 km on 75-2R. Again, this is an upper limit on the velocity as a thinner, lower velocity layer could also have been used. Beyond 56 km on the 75-2 model travel time curve, head wave arrivals from the deepest interface appear as first arrivals, corresponding to the weak first arrival of shot 54 (Fig. 4.1). However, this interface is still shown as questionable since the data could be satisfied without it by varying the overlying layers slightly.

Steeper dips were necessary on the east side of the basin for profiles 75-2 and 75-2R than for 75-3 and 75-3R to achieve the very high apparent velocity required for the last branch of 75-2R, which is still not satisfied. Steepening the dip even more would certainly fit the travel times better but since the last two shots of the profile were inadvertently

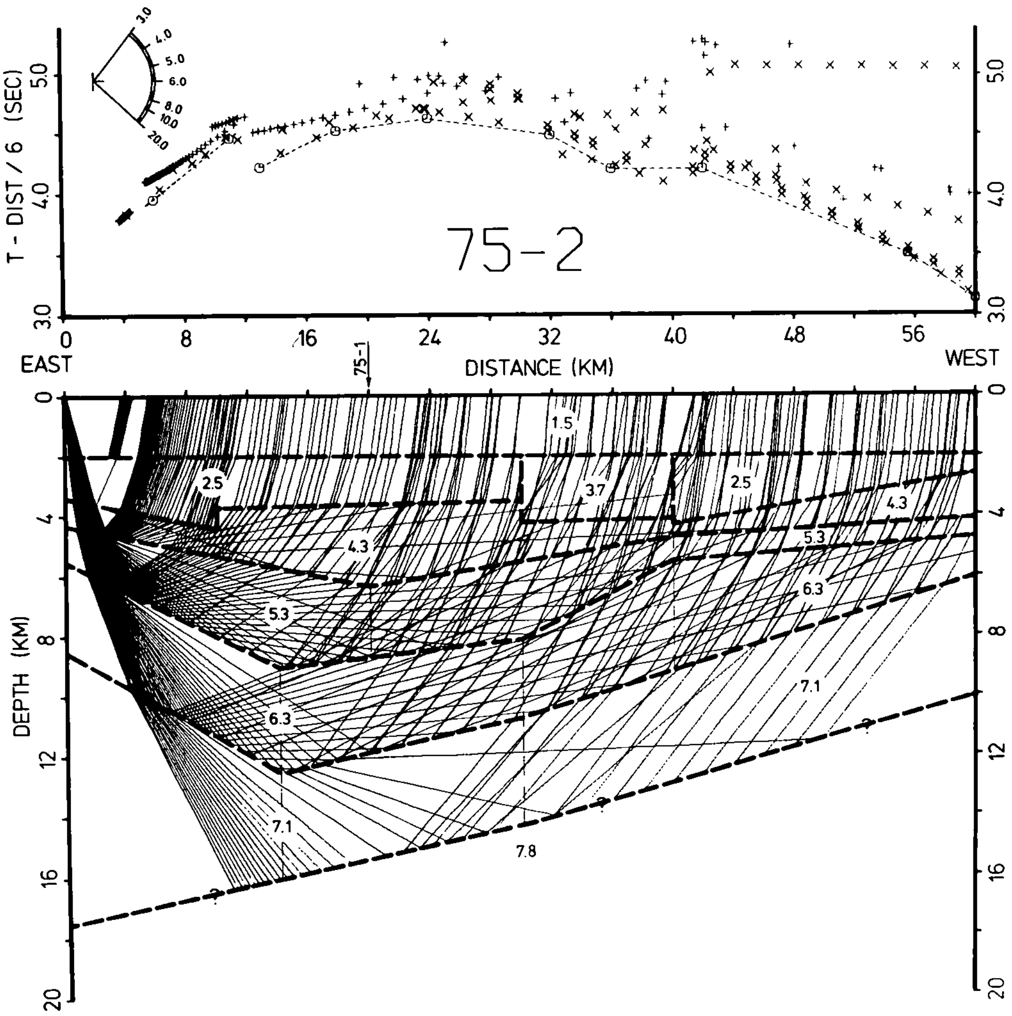

Fig. 4.10 Ray plot and travel time curve for 75-2 final model. Numbers within blocks outlined by heavy dashed lines are velocities in km/s. Vertical exaggeration is 2X.

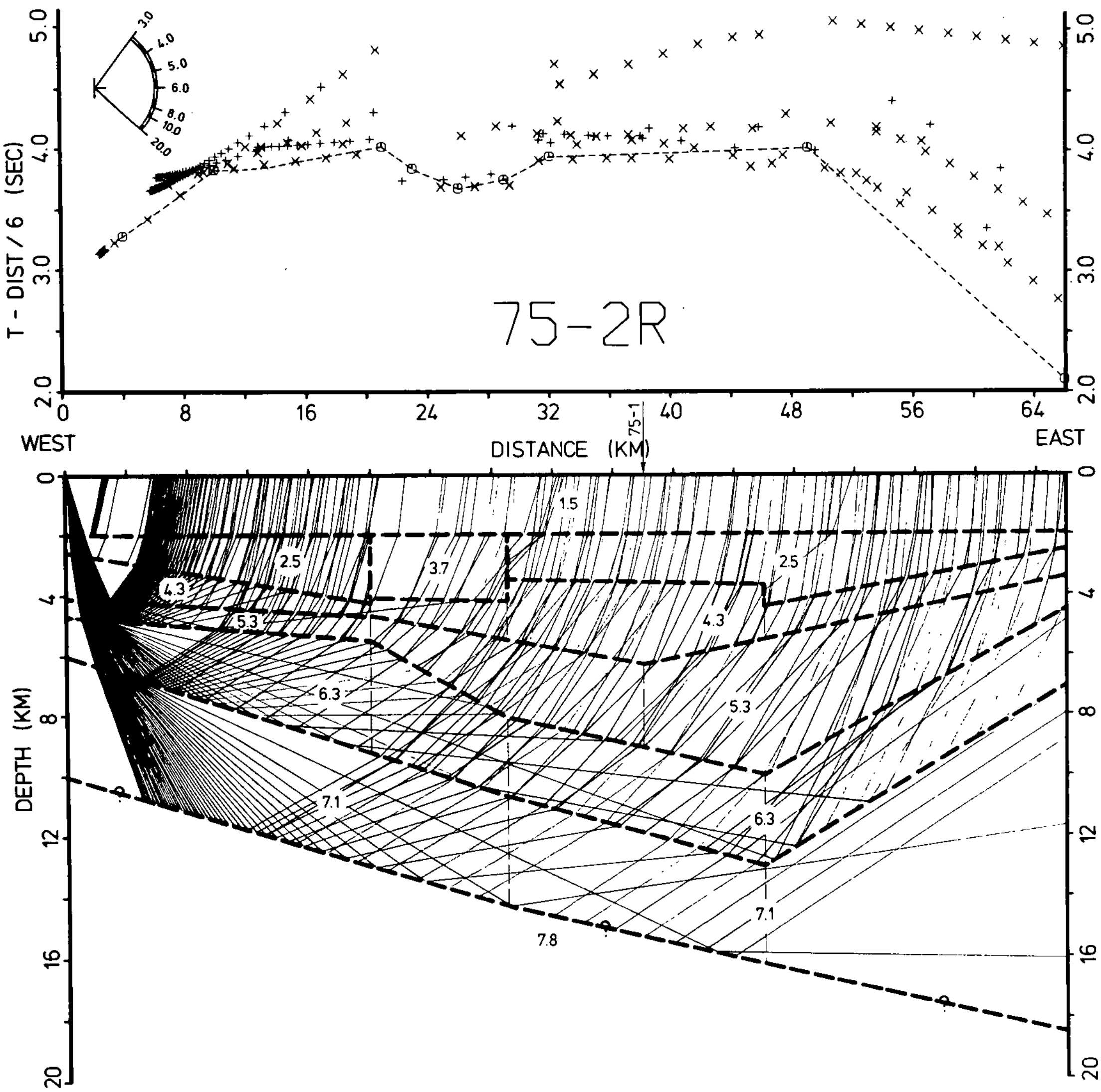

Fig. 4.11 Ray plot and travel time curve for 75-2R final model. The model is identical to 75-2 except for differences arising from the two profiles not being exactly coincident. Note that the model is reversed, west being on the left, compared with Fig. 4.10.

shot over the continental shelf the large topographic corrections required may be in error. For this reason and also because the dip already seemed steep, no further changes were made.

The amplitudes on the record sections for profiles 75-2 and 75-2R do not show as much variation as for 75-3 and 75-3R. However, the concentrations of arrivals on the model travel time curves do seem to agree in general with the observed results. For profile 75-2 the head wave branch from 12 to 16 km corresponds to the weak first arrivals observed there and the large amplitudes past 44 km correspond to the simultaneous arrival of two head wave branches. For profile 75-2R the model arrivals are very uniform out to 30 km, becoming more concentrated and extended from 30 to 48 km, in good agreement with the observed amplitudes. Beyond 48 km however, the amplitudes are smaller than would be expected from the concentration of arrivals on the model travel time curve. This is possibly an effect of the continental shelf and slope over which this part of the profile was shot.

The final models presented are by no means unique. Other combinations of layers could be found which would satisfy the travel times equally well. However, by restricting layer velocities to accepted values for similar crustal sections and by considering only geologically and tectonically feasible situations, it would be very difficult to arrive at other suitable models which would not have the same gross properties.

5. DISCUSSION

5.1 SEDIMENTS

Very recently the results of an extensive set of reflection profiles taken in 1972 off the west coast of Vancouver Island were made available to us by Chevron Standard Ltd. of Calgary. Several of the 2400% coverage air-gun profiles were shot over parts of Winona Basin, and the stacked record sections show much deeper penetration and far more detail than our reflection profiles. However the velocity-depth information determined from our profiles is more accurate because our shot-to-receiver distances ranged from 0.5 to 4.5 km while the Chevron data were collected using a multichannel streamer of less than 2 km length.

One of the Chevron profiles coincides almost exactly with C.S.P. record 75-3 (Fig. 1.4) and shows 2.5 s of sediments at the location of profile 75-3V, almost 2 s more than our profile shows. Down to 0.6 s the sediments appear flat lying and undisturbed, but beyond this they are folded and deformed possibly explaining why there is little penetration beyond 0.6 s on both 75-3V and C.S.P. record 75-3. Towards the continent much thicker flat lying sediments occur at the foot of the continental slope corresponding to the thick sediment region of C.S.P. record 75-3. Whereas only 0.9 s of sediments are indicated on the C.S.P. record, 2.7 s of very strong reflections are obvious on the Chevron section. From a preliminary and simple NMO analysis, Chevron has interpreted a similar section as consisting of 1.3 km of 2.05 km/s average velocity material overlying 2.5 km of 3.7 km/s average velocity material. These sediments are truncated sharply by a deep vertical fault at the foot of the continental slope. To the east, 0.5 s of relatively undisturbed sediments overly up to 2 s of deformed sediments. This agrees well with reflection profile 75-3 which shows only one clear reflection 0.5 s beyond the water bottom arrival. The Chevron section indicates a dip of 4°- 6° indicating a velocity of 2.6 - 2.7 km/s and a thickness of 0.8 km for this sequence (see Table II). To the southwest the Chevron section clearly shows the volcanic basement beneath 0.7 s of sediments on Paul Revere Ridge, in very good agreement with reflection profile 75-3R. The basement can easily be followed dipping beneath 1.5 s of sediments to the east of Paul Revere Ridge before becoming obscured by at least 1.3 s of deformed sediments beneath Winona Ridge.

No other Chevron profile is coincident with those in this study although two others were shot over the eastern part of the basin, one 10 km south of and parallel to profile 75-2R and another 10 km north of and parallel to 75-2. As with the first Chevron profile, up to 3 s of sediments are truncated on the east by a deep vertical fault at the foot of the continental slope. To the east of this, approximately 0.5 s of relatively undisturbed sediments overly up to 2 s of deformed sediments. This is consistent with profile 75-2 (Fig. 3.5), which shows one correlatable reflection 0.5 s after the bottom reflection. As discussed in section 3.3, profile 75-2V (Fig. 3.1), over the central part of the basin, shows four reflectors within 1.3 s of the sea-floor arrival as well as one deeper correlatable reflection (E) and one just before the bottom multiple. This corresponds well with the Chevron data. A series of strong reflections to traveltimes of about 5.5 s are shown clearly, and, as mentioned above, a preliminary analysis gave 1.3 km of material with average velocity of 2.05 km/s. This gives a 2-way traveltime of 1.3 s. Deeper in the section, Chevron's data indicate 2.5 km of 3.6 km/s sediments. The interval velocity of reflector E (Table I) is 3.63 km/s while the suggested deep reflector is at a traveltime of 5.3 s.

Another Chevron profile 25 km to the northwest of and parallel to profile 75-2 shows 0.7 s of sediments overlying volcanic basement at Paul Revere Ridge, in good agreement with reflection profile 75-2R. The basement dips beneath 2 s of relatively undeformed sediments before becoming obscured by up to 2 s of folded sediments which represent the buried northern extension of Winona Ridge.

In summary, the Chevron profiles clearly show a steady increase in sediment thickness from a few hundred meters at Paul Revere Ridge to about 4 km at the foot of the continental slope. This is in qualitative agreement with the 4 - 6 km thickness predicted by Couch (1969) on the basis of gravity data. Several features of the sections, particularly the deformed sediments of Winona Ridge appear to be the result of northeast-southwest compression. This could be caused by either slow convergence of the Explorer-American plates or subduction of the Explorer plate beneath the American plate. The vertical fault at the foot of the continental slope is similar to that observed on C.S.P. records off the west coast of the Queen Charlotte Islands (Chase et al, 1975) and could indicate a component of lateral motion resulting from oblique subduction.

5.2 RAY TRACING MODELS

Before discussing the tectonic implications of the ray tracing models, a few words should be said about the resolution to be expected for the various layers. As mentioned previously, the only constraints which apply to the entire crust are those obtained from refraction profiles 75-1 and 75-1R. The uncertainty in the positions of these layers is of the order of 1 - 2 km. The remainder of the models is non-unique and depends on preconceived notions of tectonic structure. The deeper layers have been chosen primarily to satisfy travel times and variations in their positions are possible. The first few layers at the ends of the models are required to fit the travel times at the start of the profiles and if the velocities from 75-1,1R are to be assumed they cannot vary too much. Of course this assumption would be invalid if significant horizontal velocity gradients are present.

In light of the data recently acquired from Chevron, it appears at first glance that the sediment layer chosen is too thin. However a re-examination of profile 75-1,1R results shows that the 4.3 km/s layer that Lynch (1977) interpreted extends from 2.2 to 2.8 s beyond the water bottom arrival. One of the Chevron profiles runs approximately 5 km to the southeast of and parallel to profile 75-1R and shows definite sedimentary layering over the entire profile length for this time interval. At this depth of burial it is not unreasonable for sediments to have a velocity of 4.3 km/s. Thus both the 2.5 and the 4.3 km/s layers constitute sediments on the ray tracing models.

A velocity of 3.7 km/s has been chosen for Winona Ridge although making this layer thinner would have made possible the use of a lower velocity. This implies that the velocity of the ridge is likely not greater than 3.7 km/s, indicative of a higher velocity sediment than the surrounding sediments and which could have resulted from compression.

The most striking, and probably the most important feature of the models is the westward dipping layers on the east side of the basin. These are required to satisfy the very high apparent velocities on the travel time curves of 75-2R and 75-3R. The deepest point of the layers could be shifted by up to 5 km to either side and still satisfy the travel times, but no configuration of layers dipping to the east would be possible without introducing horizontal velocity gradients. Since this part of both models is under the continental slope it could represent a transition from oceanic to continental crust over this distance. However, in going from oceanic to continental crust a negative horizontal gradient, contrary to the model, would be expected.

Regardless of the layer boundaries shown, there must be a more rapid overall increase in velocity with depth for the sides of the basin than for the center in order to satisfy the travel times. The eastward dipping crust on the west side of the models suggests a subducting plate. Perhaps the westward dipping layers on the east side of the basin represent a buckling of the crust in response to a recent initiation of subduction or increase in subduction rate in this area.

In order that the models be acceptable, they must be consistent with the gravity data. To check this, Clowes and Whittall (personal communication, 1978) have performed a preliminary gravity calculation for model 75-3 to compare with the free air anomaly. Although much more work is necessary to remove unwanted end effects they have shown that the model is capable of satisfying the data.

5.3 TECTONIC SIGNIFICANCE OF WINONA BASIN

The results of this project, coupled with existing geophysical and geological information, suggest that oblique subduction could be occurring at Winona Basin. If, as has been hypothesized by some authors (ie. Riddihough, 1977; Murray and Tiffin, 1974), the triple junction has recently (within the past 4 m.y.) migrated from the Brooks Peninsula area to the Dellwood Knolls, (Figs. 1.1 & 1.2) the subduction zone would also have had to make a corresponding shift to the northwest. As pointed out by Riddihough (1977) convergence of the Explorer and American plates has been oblique and very slow (1.9 to 1.4 cm/yr) over the past 3 m.y.; consequently convergence without subduction is possible since the young crust is presumably still warm and perhaps unable to subduct. However if there has been a slight component of oblique subduction along the Queen Charlotte transform fault, a subducting plate would already have been established prior to the triple junction shift. The thick sediment-filled trough with evidence of northeast-southwest compression and the bowl like structure of the deeper crust in Winona Basin are strong evidence for subduction. The westward dipping layers on the east side of the basin could represent buckling of the crust in response to an increase in the convergence rate following the triple junction shift. Similarly the deep vertical fault at the foot of the continental slope indicates a definite component of lateral motion. These observations are best explained by oblique subduction between the Explorer and American plates.

In order to get a complete understanding of the structure of Winona Basin and the tectonic forces operating on it, more geophysical information is needed. However the results of this study place important constraints on the overall picture and any conclusions made must be consistent with them.

REFERENCES

Cerveny, V. and R. Ravindra 1971. Theory of Seismic Head Waves. University of Toronto Press, 312 pp.

Chase, R.L., D.L. Tiffin and J.W. Murray 1975. The western Canadian continental margin. Canadian Society of Petroleum Geologists, Memoir 4, pp. 701-721.

Clayton, R.W. 1975. The deconvolution of teleseismic recordings. Unpublished M.Sc. thesis, University of British Columbia.

Clee, T.E., K.G. Barr and M.J. Berry 1974. Fine structure of the crust near Yellowknife. Can. J. Earth Sci. 11, pp. 1534-1549.

Clowes, R.M. 1977. A marine deep seismic sounding system. Can. J. Earth Sci. 14, pp. 1276-1285.

Couch, R.W. 1969. Gravity and structures of the crust and sub-crust in the northeast Pacific ocean west of Washington and British Columbia. Unpublished PhD. thesis, Oregon State University, Corvallis, OR.

Dix, C.H. 1955. Seismic velocities from surface measurements. Geophysics 20, pp. 68-86.

Grubbe, K. 1976. Seismic-refraction measurements along two crossing profiles in northern Germany and their interpretation by a ray-tracing method. In: Explosion Seismology in Central Europe. P. Giese, C. Prodehl and A. Stein (eds.), Springer-Verlag, Berlin 1976, pp. 268-282.

Kanasewich, E.R. 1976. Time Series Analysis in Geophysics, 2nd ed., University of Alberta Press, 352 pp.

Kramer, F.S., R.A. Peterson and W.C. Walter 1968. Seismic energy sources handbook, 1968. United Geophysical Corporation, 57 pp.

Lynch, S. 1977. The crustal structure of Winona Basin as determined by deep seismic sounding. Unpublished M.Sc. thesis, University of British Columbia.

Miller, H. and H. Gebrande 1976. Crustal structure in southeastern Bavaria derived from seismic-refraction measurements by ray-tracing methods. In: Explosion Seismology in Central Europe. P. Giese, C. Prodehl and A. Stein (eds.), Springer-Verlag, Berlin 1976, pp. 339-346.

Mota, L. 1954. Determination of dips and depths of geological layers by the seismic refraction method. Geophysics 19, pp. 242-254.

Muller, St., A. Stein and R. Veis 1962. Seismic scaling laws for explosions on a lake bottom. Zeit. f. Geophys. 28, pp. 258-280.

Murray, J.W. and D.L. Tiffin 1974. Patterns of deformation, sedimentation and tectonism, southwestern Canadian continental margin. Ann. de la Soc. Geol. de Belgique 97, pp. 169-183.

O'Brien, P.N.S. 1960. Seismic energy from explosions. Geophys. J.R. astr. Soc. 3, pp. 29-44.

Riddihough, R.P. and R.D. Hyndman 1976. Canada's active western margin - the case for subduction. Geosci. Canada 3, pp. 269-278.

Riddihough, R.P. 1977. A model for recent plate interactions off Canada's west coast. Can. J. Earth Sci. 14, pp. 384-396.

Shor, G.G., Jr. 1963. Refraction and reflection techniques and procedure. In: The Sea. M.N. Hill (ed.), Interscience, New York, pp. 20-38.

Telford, W.M., L.P. Geldart, R.E. Sheriff and D.A. Keys 1976. Applied Geophysics. Cambridge University Press, Cambridge, 860 pp.

Tiffin, D.L., B.E.B. Cameron and J.W. Murray 1972. Tectonics and depositional history of the continental margin off Vancouver Island, British Columbia. Can. J. Earth Sci. 9, pp. 280-296.

Tiffin, D.L. and D. Seeman 1975. Bathymetric map of the continental margin of western Canada. Open file map, Geol. Surv. of Canada.

Wiggins, R.A. 1976. Body wave amplitude calculations II. Geophys. J.R. astr. Soc. 46, pp. 1-10.

Wiggins, R.A. 1977. Minimum entropy deconvolution. Proceedings of the International Symposium on Computer Aided Seismic Analysis and Discrimination, June 9 & 10, 1977, Falmouth, Mass., IEEE Computer Society, pp. 7-14.

Wood, L.C., R.C. Heiser, S. Treitel and P.L. Riley 1978. The debubbling of marine source signatures. Geophysics 43, pp. 715-729.